GEOMAR REPORT

GEOMAR

Helmholtz-Zentrum für Ozeanforschung Kiel

RV MARIA S. MERIAN Fahrtbericht / Cruise Report MSM78

PERMO 2

Edinburgh – Edinburgh (U.K.)
16.10. – 25.10.2018

Berichte aus dem GEOMAR
Helmholtz-Zentrum für Ozeanforschung Kiel

Nr. 48 (N. Ser.)

February 2019

GEOMAR

Helmholtz-Zentrum für Ozeanforschung Kiel

RV MARIA S. MERIAN Fahrtbericht / Cruise Report MSM78

PERMO 2

Edinburgh – Edinburgh (U.K.)
16.10. – 25.10.2018

Berichte aus dem GEOMAR
Helmholtz-Zentrum für Ozeanforschung Kiel

Nr. 48 (N. Ser.)

February 2019

GEOMAR
Helmholtz-Zentrum für Ozeanforschung Kiel

Das GEOMAR Helmholtz-Zentrum für Ozeanforschung Kiel ist Mitglied der Helmholtz-Gemeinschaft Deutscher Forschungszentren e.V.

The GEOMAR Helmholtz Centre for Ocean Research Kiel is a member of the Helmholtz Association of German Research Centres

Herausgeber / Editors:
Jens Karstens, Christoph Böttner, Mike Edwards, Ismael Falcon-Suarez, Anita Flohr, Rachael James, Anna Lichtschlag, Doris Maicher, Iain Pheasant, Ben Roche, Bettina Schramm, Michael Wilson

GEOMAR Report
ISSN Nr.. 2193-8113, DOI 10.3289/GEOMAR_REP_NS_48_2019

Helmholtz-Zentrum für Ozeanforschung Kiel / Helmholtz Centre for Ocean Research Kiel
GEOMAR
Dienstgebäude Westufer / West Shore Building
Düsternbrooker Weg 20
D-24105 Kiel
Germany

Helmholtz-Zentrum für Ozeanforschung Kiel / Helmholtz Centre for Ocean Research Kiel
GEOMAR
Dienstgebäude Ostufer / East Shore Building
Wischhofstr. 1-3
D-24148 Kiel
Germany

Tel.: +49 431 600-0
Fax: +49 431 600-2805
www.geomar.de

Table of content

1 Cruise Summary

1.1 German

Der Fluidfluss in Sedimentbecken wird in erster Linie durch die hydraulischen Eigenschaften, insbesondere die Permeabilität, der Sedimente kontrolliert. Wird der Fluidfluss durch Permeabilitätsbarrieren gehindert, so können sich Überdrücke akkumulieren, die zur Entstehung von fokussierten Fluidwegsamkeiten führen können. Das Freisetzen der Fluide führt zur Entstehung von „Pipe“-Strukturen, die in seismischen und hydroakustischen Daten gut sichtbar sind und sich am Meeresboden durch Krater, die in diesem Zusammenhang als Pockmarks bezeichnet werden, manifestieren können.

Das durch die Europäische Kommission im Rahmen des Arbeitspakets 3 des Horizon 2020 Programmes geförderte Projekt „Strategies for Environmental Monitoring of Marine Carbon Capture and Storage“ (STEMM-CCS) hat das Ziel die Permeabilität solcher natürlichen Fluidflussstrukturen zu bestimmen und so eine bessere Risikoabschätzung für die submarine CO_2-Speicherung zu ermöglichen. Hierfür fand im Mai 2017 eine erste wissenschaftliche Ausfahrt MSM63 zur Scanner Pockmark im britischen Sektor der Nordsee statt, um diese und die darunterliegende Pipe-Struktur seismisch, hydroakustische und elektromagnetisch zu untersuchen. Im Rahmen dieser Kampagne sollte diese Struktur zusätzlich durch das Meeresbodenbohrgerät RockDrill2 erbohrt werden, um mit Hilfe von Sedimentproben die hydraulischen Eigenschaften der Sedimente zu bestimmen und die geophysikalischen Messungen zu validieren. Diese Experimente konnten 2017 auf Grund technischer Probleme am Schiff nicht durchgeführt werden und die Expedition MSM78 diente dem Nachholen des verhinderten Forschungsprogramms..

Die Expedition MSM78 fand vom 16.10.2018 bis zum 25.10.2018 statt. Die Arbeiten begannen mit hydroakustischen Messungen und Kartierungen des Meeresbodens (Sedimentecholot und Fächerecholot). Ein viertägiges Wetterfenster ermöglichte einen kontinuierlichen Einsatz des RockDrill2, während dessen vier Kerne mit insgesamt 22.6 m an Kernmaterial gezogen werden konnten. Daraufhin erlaubte starker Wellengang und Wind für zweieinhalb Tage nur noch hydroakustische Messungen. Am Ende der Expeditionen wurden zusätzlich noch 29.6 m an Schwerelotkernen gezogen. Auf Grund der kurzen Dauer der Expeditionen wurden lediglich Porenwasserproben genommen und die Kerne für den Transport aufbereitet. Eine Auswertung wird erst später an Land stattfinden.

1.2 English

Fluid flow in sedimentary basins is primarily controlled by the hydraulic properties, especially the permeability, of the sediments. The presence of permeability barriers may lead to the accumulation of pore fluid overpressure, which may cause the formation of focused fluid conduits. The focused release of fluids causes the formation of pipe structures, which can be imaged with seismic and hydroacoustic techniques. Such fluid release may manifest as crater structures, known as pockmarks, at the seafloor.

The European Commission funded Horizon 2020 (Work package 3) project „Strategies for Environmental Monitoring of Marine Carbon Capture and Storage“ (STEMM-CCS) has the goal to determine the permeability of natural fluid flow structures, which allows a more reliable risk assessment for the storage of CO_2 beneath the seafloor. For this purpose, a first scientific (MSM63) targeted the Scanner Pockmark (British Sector of the North Sea) During MSM63 conducted several seismic, hydroacoustic, and controlled source electromagnetic experiments were conducted. Originally, these experiments should have been accompanied by drilling into the fluid flow structures using the seafloor-

drilling device RockDrill2. However, due to technical problems of the vessel, these experiments could not be accomplished during MSM63 in 2017 and were rescheduled for MSM78.

The expedition MSM78 took place from the 16th until the 25th of October 2018. The scientific program started with hydroacoustic measurements and mapping (sediment echosounder and multibeam echosounder). Calm weather conditions allowed the usage of RockDrill2 for four consecutive days, during which a total of 22.6 m of sediment core material could be recovered. After this, weather conditions became worse only allowing hydroacoustic measurements for two-and-a-half days. Finally, we could core in total 29.6 m of sediments using a gravity corer. Due to the limited duration of the cruise, only pore water samples were obtained and the core material was prepared for transport. All analysis will be conducted onshore.

2 Participants

2.1 Scientific Party

1.	Dr. Jens Karstens	Chief scientist	GEOMAR
2.	Christoph Böttner	Hydroacoustics	GEOMAR
3.	Bettina Schramm	Hydroacoustics	GEOMAR
4.	Rebecca Kühn	Hydroacoustics	GEOMAR
5.	Michael Wilson	RockDrill2	BGS
6.	Will Lewis	RockDrill2	BGS
7.	David Baxter	RockDrill2	BGS
8.	Iain Pheasant	RockDrill2	BGS
9.	Apostolos Tsiligiannis	RockDrill2	BGS
10.	Rodrique Akkari	RockDrill2	BGS
11.	David Bailey	RockDrill2	BGS
12.	Paul Kane	RockDrill2	BGS
13.	Ewan Brown	RockDrill2	BGS
14.	Dr. Anna Lichtschlag	Marine geochemistry	NOCS
15.	Dr. Anita Flohr	Marine geochemistry	Soton
16.	Mike Edwards	Sediment coring	NOCS
17.	Dr. Ismael Falcon-Suarez	Marine geochemistry	NOCS
18.	Ben Roche	Hydroacoustics	NOCS
19.	Prof. Dr. Rachael James	Marine geochemistry	Soton
20.	Dr. Doris Maicher	Sediment coring	GEOMAR
21.	Frank Stephan Rahn	Technician ship maintenance	Sauer & Sohn
22.	Steven Billowie	Technician ship maintenance	Sauer & Sohn

2.2 Affiliations

GEOMAR	GEOMAR Helmholtz Centre for Ocean Research Kiel Marine Geodynamics, Wischhofstr. 1-3, 24148 Kiel, Germany
BGS	British Geological Survey, The Sir George Bruce Building, Research Avenue South, Edinburgh, EH14 4AP, U.K.
NOCS	National Oceanography Centre, European Way, Southampton SO14 3ZH, U.K.

Soton	University of Southampton, European Way, SO14 3ZH, Southampton, U.K.
Sauer & Sohn	J.P. Sauer & Sohn Maschinenbau GmbH, Brauner Berg 15, 24159 Kiel, Germany

2.3 Crew

1.	Ralf Schmidt	Master
2.	Björn Maaß	Chief Officer
3.	Sören Janssen	1st Officer
4.	Sandra Schilling	2nd Officer
5.	Thomas Ogrodnik	Chief Engineer
6.	David Woltemade	2nd Engineer
7.	Philipp Schwieder	3rd Engineer
8.	Michael Maggiulli	System Operator
9.	Jörg Walter	Electronics
10.	Frank Baumann	Electrician
11.	Jürgen Sauer	Oiler
12.	Helmut Friesenborg	Fitter
13.	Enno Vredenborg	Bosun
14.	Andre Werner	Ships Mechanic
15.	Olaf Bischeck	Ships Mechanic
16.	Peter Peschkes	Ships Mechanic
17.	Karsten Peters	Ships Mechanic
18.	Felix Meyer	Ships Mechanic
19.	Sebastian Plink	Ships Mechanic
20.	Andreas Schrapel	Ships Mechanic
21.	Sebastian Matter	1st Cook
22.	Georg Preuß	2nd Cook
23.	Sylvia Kluge	Stewardess
24.	Dr. Ludwig Staak	Ship’s Doctor

3 Research Program

3.1 Motivation

The research cruise MSM78 is part of STEMM-CCS projects and its main aim is to collect sediment cores for geochemical and geotechnical analyses. These experiments were originally planned for the second leg of research cruise MSM63 in May 2017, but could not be realized due to technical problems of the vessel. The motivation for MSM78 was identical to MSM63 (Berndt et al., 2017) and was summarized in the cruise report of MSM63 as follows:

Young marine sediments may have porosities in excess of 90%. During burial sediments in marine sedimentary basins compact and porosity reduces to less than 10% in several kilometers depth releasing enormous amounts of pore fluid. The transport of fluids through marine sediments is primarily governed by pressure and permeability contrasts. The past three decades have completely overturned the way in

which we think about this fluid migration. While in the past, it was assumed that fluid migration is diffusive by migration through permeable beds, which can be described by Darcy's law, three-dimensional (3D) seismic data have revealed an enormous range of anomalies that can be related to focused fluid migration. This focusing occurs whenever the escape of fluids from the sediments cannot keep up with the forces driving the fluids out of the sediments, e.g. rapid loading, hydrothermal activity, or diagenetic processes and is primarily directed up to the surface of the basin. The formation of pathways is generally believed to be controlled by overpressure-induced hydro fracturing of an impermeable cap rock and fluid migration, but it is not known how long after formation they remain open and how permeable they are compared to the generally low permeability of the host sediments. By altering the integrity of sealing cap rocks and transferring pressure in the marine sedimentary overburden, vertical fluid conduits imply inter-stratigraphic hydraulic connectivity and significantly affect the migration of fluids and gases in the subsurface [Karstens & Berndt, 2015]. Emergence, architecture and mechanics of vertical fluid migration structures require a fundamental understanding as they might affect the transmission of fluids and gases from the sedimentary strata to the hydrosphere and finally to the atmosphere [Gurevich et al., 1993; Gasda et al., 2004]. Apart from direct geological implications, such as climate controls or slope stability, focused fluid migration affects severely safety and efficiency of exploration wellbore activities and sub-seabed CO2 storage operations in marine sedimentary basins and thus needs to be understood in detail to minimize potential hazards.

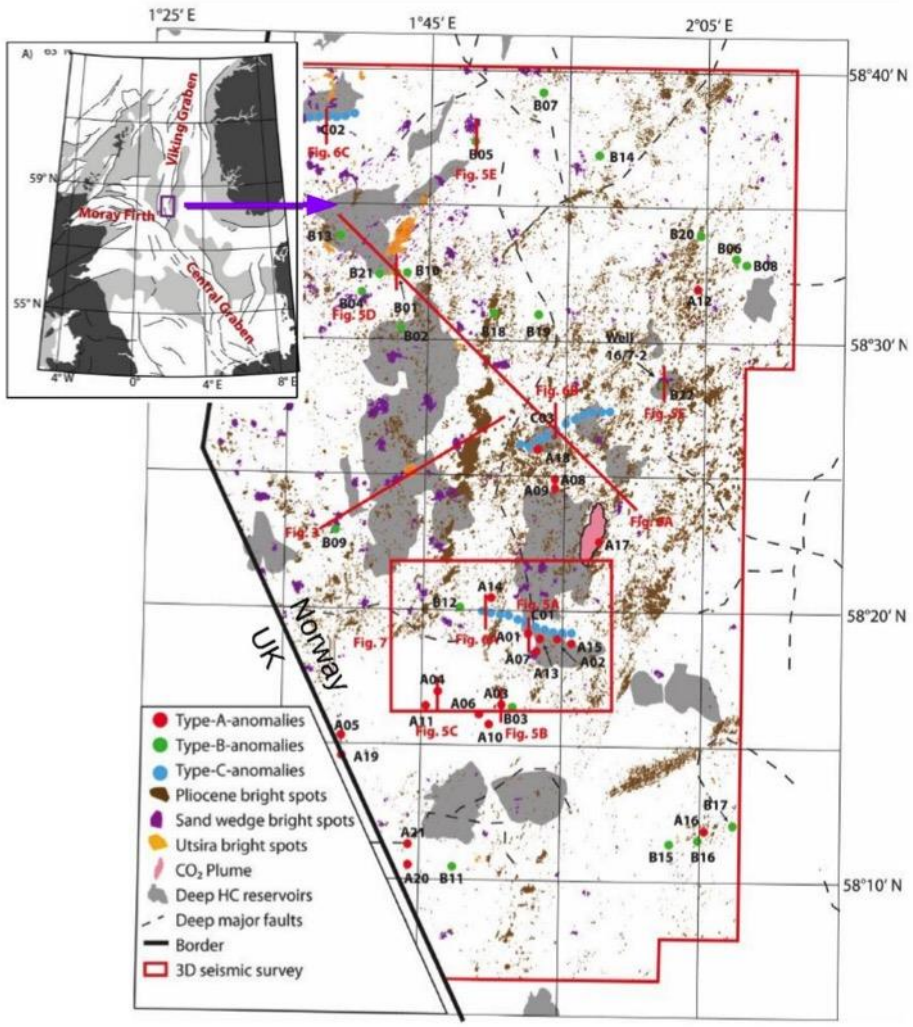

Figure 1: Map of the Sleipner area in the Southern Viking Graben showing the location of fluid flow manifestations and exploration type seismic profiles (red lines): bright spots beneath the top of the

Utsira Formation (pale green), within the sand wedge (pale red), beneath the top Pliocene (pale blue), type-A-anomalies (red dots), type-B-anomalies (green dots), type-C-anomalies (red dots), CO2-plume (rose), deep hydrocarbon reservoirs (grey), deep faults (dashed black lines) [Karstens, 2015]

Different studies and geophysical field programs on focused fluid flow structures have been conducted in the past and will be supplemented by the scientific objectives of this proposal. The 7th framework European Union funded research project "ECO2 – Sub-seabed CO_2 Storage: Impact on Marine Ecosystems" successfully published it's summary report in April 2015 with a new approach regarding the environmental risk assessment for sub-seabed storage sites of carbon capture and storage (CCS) projects. ECO2 was triggered by the activities of several EU supported demonstration projects to store CO_2 at the emergence of fossil fuel power plants into either marine sub-seabed storage sites or onshore deep geological formations. Within the industrial countries, CCS is regarded as a key technology to significantly reduce CO_2 emissions from new and existing industrial sources and mitigate the contribution of greenhouse gas emissions to global warming and ocean acidification. In particular, the injection into oil-, gas- or water-bearing geological storage sites is regarded as a suitable option for carbon dioxide sequestration on a commercial scale. ECO2 conducted a comprehensive offshore field programme at the Norwegian storage sites Sleipner and Snøvit and at several natural CO_2 seepage sites in order to identify potential pathways for CO_2 leakage through the overburden and to monitor and track their fluid flux in the seabed and water column. The key objectives addressed by ECO2 were to investigate the likelihood of leakage from sub-seabed storage sites, understand the potential effects on benthic ecosystems and finally assess the risk of sub-seabed carbon dioxide storage sites. The objectives were followed by numerous field campaigns, research cruises, laboratory experiments and numerical modelling [ECO2, 2015]. As one of the main results the investigations of ECO2 revealed that a quantitative assessment of CO_2 seepage rates and a reliable prediction of seep sites cannot be conducted unless the nature, and in particular the permeability of sub-seabed chimney structures is better constrained.

During his PhD thesis [Karstens, 2015] Jens Karstens of GEOMAR mapped, quantified and interpreted focused fluid conduits in the marine sedimentary basin of the Sleipner area in the North Sea Basin in the exploration type 3D seismic data set ST98M3, acquired by Statoil. Research on the Sleipner CO_2 storage site has mainly focused on the CO_2 migration within the storage formation [e.g. Chadwick et al., 2009; Arts et al., 2008], while natural fluid manifestations in the overburden have only been reported briefly by Heggland [1998] and Nicoll [2011]. The investigated industrial data cover an area of 2,000 km^2 and were processed with 12.5 m horizontal and ~10 m vertical resolution. Karstens mapped and categorized vertical seismic anomalies (Figure 3.1.1, type-A-anomalies, type-B-anomalies, type-C-anomalies). In total, 46 large-scale vertical seismic anomalies (500–800 m long and 100-1000 m wide) are present in the shallow (> 1000) subsurface of the study area and their appearance assigned to different formation processes (Figure 3.1.1). These seismically imaged chimneys are considered to be pathways for sedimentary fluid flow, which could act as pathways for CO2, if the plume reaches the base of the structures and if their permeability is high enough. The analyses revealed seal-weakening, formation-wide overpressure and the presence of free gas as the requirements to initiate the formation of vertical fluid conduits in the Southern Viking Graben [Karstens & Bendt, 2015].

Similar seismic anomalies have been recognized around the world and are generally associated with vertical fluid flow [e.g. Berndt, 2005; Cartwright et al., 2007; Løseth et al., 2009; Andresen, 2012; Gay et al., 2012]. The activity of vertical fluid conduits can be associated to blowout-like events, e.g. resulting in pipe structures offshore Nigeria [Løseth et al., 2011] or Norway [Bünz et al., 2003] or fluid flow may be continuous and long-lasting, e.g. chimney structures above North Sea salt diapirs [Hovland and Sommerville, 1985; Granli et al., 1999; Arntsen et al., 2007]. The shallow subsurface of the Central North Sea is highly affected by focused fluid flow. The seafloor of the Fladen Ground in the British

sector west of the Sleipner area is densely populated with pockmarks. Most of these pockmarks are only a few meters wide, while a few prominent structures like the Scanner Pockmark have diameters of more than 100 meter [Judd and Hovland, 2007]. The Scanner Pockmark emits methane, which is trapped beneath a glacial unconformity less than 80 meters below the seafloor [Judd et al., 1994]. 3D seismic data suggest that this shallow gas reservoir is charged by a vertical fluid conduit comparable to the seismic fluid flow structures identified in the Sleipner area (Figure 2 left).

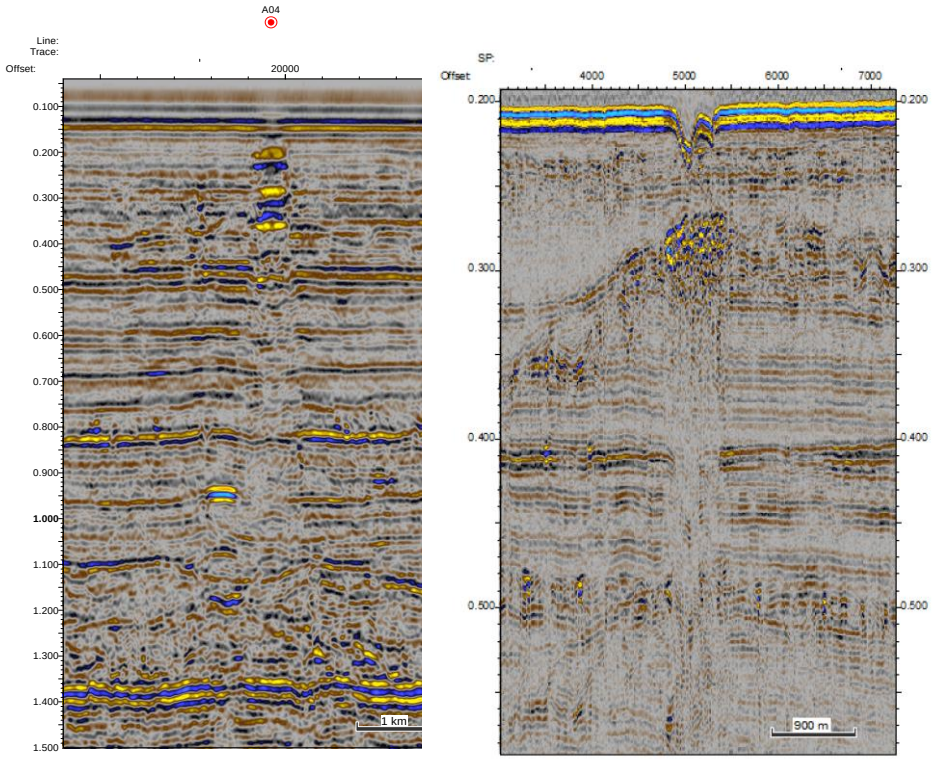

Figure 2: Seismic examples for pipe structures. The left panel shows exploration type 3D seismic data of Chimney A04 south of the Sleipner Field. The right panel shows the pipe structure underlying the Scanner Pockmark in high-resolution 2D seismic data collected during MSM63.

We selected the two prominent vertical seismic fluid flow structures A04 (Sleipner area, Norway) and the Scanner Pockmark (U.K.) in the Southern Viking Graben as study sites for this cruise. Both structures have been imaged previously with exploration-type 3D seismic data and were judged suitable for our experiments (Figures 2, right and left). However, the 3D seismic data could not resolve if the fluid conduit of A04 crosscuts the youngest glacial sediments and would be reachable with drilling. Therefore, the final site selection for the Scanner Pockmark Site depended on high-resolution sub-bottom profiler data, which we collected during the cruise. Altogether, we did acquire high-resolution 2D seismic data, very high-resolution sub-bottom profiler data to image small-scale fracture networks in the top 20 m of sediments, ocean bottom seismometer data for velocity analysis and controlled source electromagnetic data to assess fracture anisotropy in the subsurface [Exley et al., 2010; Key et al., 2012]. All four data sets will be combined to a geophysical model of a chimney structure and form the basis for permeability modelling after the data have been ground-truthed by drilling. These data will provide the steppingstone from interpretation of borehole samples to exploration-type 3D seismic data. This will provide the geophysical database for assessing the permeability of a typical chimney structure. Within the STEMM-CCS project, the analysis and interpretation of the borehole results will be augmented with the study of field analogues and numerical simulations.

3.2 Aims of the Cruise

The aims of MSM78 was identical to MSM63 and was summarized in the cruise report of MSM63 (Berndt et al., 2017) as follows:

Quantification of focused fluid migration through the sedimentary succession is fundamental for a large number of research themes ranging from the assessment of geological climate controls and slope stability to verify applied question such as where hydrocarbons accumulate and how safe CO_2 storage is [Berndt, 2005]. Within the ECO_2 project, we have attempted to assess the integrity of the overburden, but the combination of field studies and numerical simulation has shown clearly that it is not possible to describe fluid migration in a sedimentary basin quantitatively without understanding the role of seismic chimney structures.

The main scientific goals of this project were

a) **Firstly, to constrain the bulk permeability of an existing chimney structure**, i.e. to assess the amount of aqueous and gassy fluids that may move through these structures over time.
b) **Secondly, we tried to constrain the temporal evolution of fluid migration through pipe structures over time,** i.e. do they transport fluids continuously or episodically and if episodically is it likely that CO_2 storage may initiate a new episode of migration.
c) **Thirdly, we set out to test the hypothesis that chimney structures in seismic data represent indeed fault networks created by hydro-fracturing** and not bulk mobilization of sediments as a diapir or subsidence of sediments in the style of a breccia pipe.

These goals will be met within the STEMM-CCS project by combining geophysical observations from two scientific cruises by GEOMAR and the National Oceanography Centre, Southampton with field samples from California and numerical simulations. The cruise proposed here will provide the required borehole samples from inside and outside the chimney structures and the necessary geophysical data with different frequency content from high-resolution subbottom profiler data to P-Cable high-resolution data to upscale the borehole observations through a nested approach to the existing high-quality exploration-type seismic data. This will provide the required data set to achieve the three objectives above. These data will be augmented by ocean bottom seismometer data and controlled-source electro-magnetic data, which we will collect during the cruise and which will allow us determining if there is continuously linked fracture permeability inside the chimney structures from directional differences in the seismic velocities and the electric resistivity, respectively.

4 Narrative of the Cruise

16.10.2018, Tuesday

After the mobilization of the RockDrill2, we left Edinburgh harbor in the afternoon and sailed to the study area in the Central North Sea

17.10.2018, Wednesday

We reached the area covered by our research permit around 02:00 (UTC) and collected a first water sound velocity profile for calibrating the hydroacoustic experiments and started recording Parasound and EM712 data. In the afternoon, we reached the study area around the Scanner Pockmark, collected an additional water sound velocity profile, and surveyed the previously selected RockDrill2 sites. At 16:00 (UTC), we deployed RockDrill2 at the reference core location and the drilling operation started at 20:40 (UTC).

18.10.2018, Thursday

The entire day was used for continuous drilling.

19.10.2018, Friday

At 6:52 (UTC), the drilling operation was stopped after reaching a depth of 24 m below seafloor and the RockDrill2 was recovered. The obtained sediment cores were immediately cut and pore water samples were taken. During the recovery of the samples and re-equipment of the RockDrill2, we collected additional bathymetric data. Around 16:00 (UTC), RockDrill2 was deployed at the main core location within the Scanner Pockmark to conduct a drilling recovery test. Between 16:14 and 18:30 (UTC), RockDrill2 reached a depth of 3.4 m below seafloor and was recovered to evaluate the applied drilling configuration. At 22:30 (UTC), RockDrill2 was deployed again, but had a technical problem and had to be recovered.

20.10.2018, Saturday

After fixing the technical problem, RockDrill2 was deployed again at 02:00 (UTC) and drilled to a depth of 10.3 m below seafloor, which was reached at 15:20 (UTC). Afterwards, the borehole was scanned using the Optical, Acoustic and spectral Gamma logging tool and afterwards RockDrill2 was recovered around 18:00 (UTC). The obtained sediment core segments were recovered, cut and sampled. RockDrill2 was re-equipped for a final drilling operation at the reference site and deployed at 21:30. The first 31 m were drilled as an open-hole (no coring), which and was followed by coring of two sections reaching a maximum depth of 34.3 m below seafloor.

21.10.2018, Sunday

Due to technical problems with the top-drive of RockDrill2, the drilling operation had to be stopped and systems was recovered at 18:45 (UTC). In the evening, wind speed and wave height increased and it was not possible to conduct additional RockDrill2 operations. At 19:20 (UTC), we started recording additional hydroacoustic profiles.

22. 10.2018, Monday and 23.10.2018, Tuesday

The wind reached force 7 to 9 for a period of more than 50 hours and we could only collect hydroacoustic profiles following the main wave direction during this period.

24.10.2018, Wednesday

At 7:00 (UTC), we began collecting gravity cores. Five gravity cores were obtained within the Scanner Pockmark at three different sites and two at the reference core site. We recorded a final water sound velocity profile at 12:37 (UTC) and collected a final Parasound profile before sailing back to Edinburgh.

25.10.2018, Thursday

We arrived Edinburgh in the afternoon and started with the demobilization.

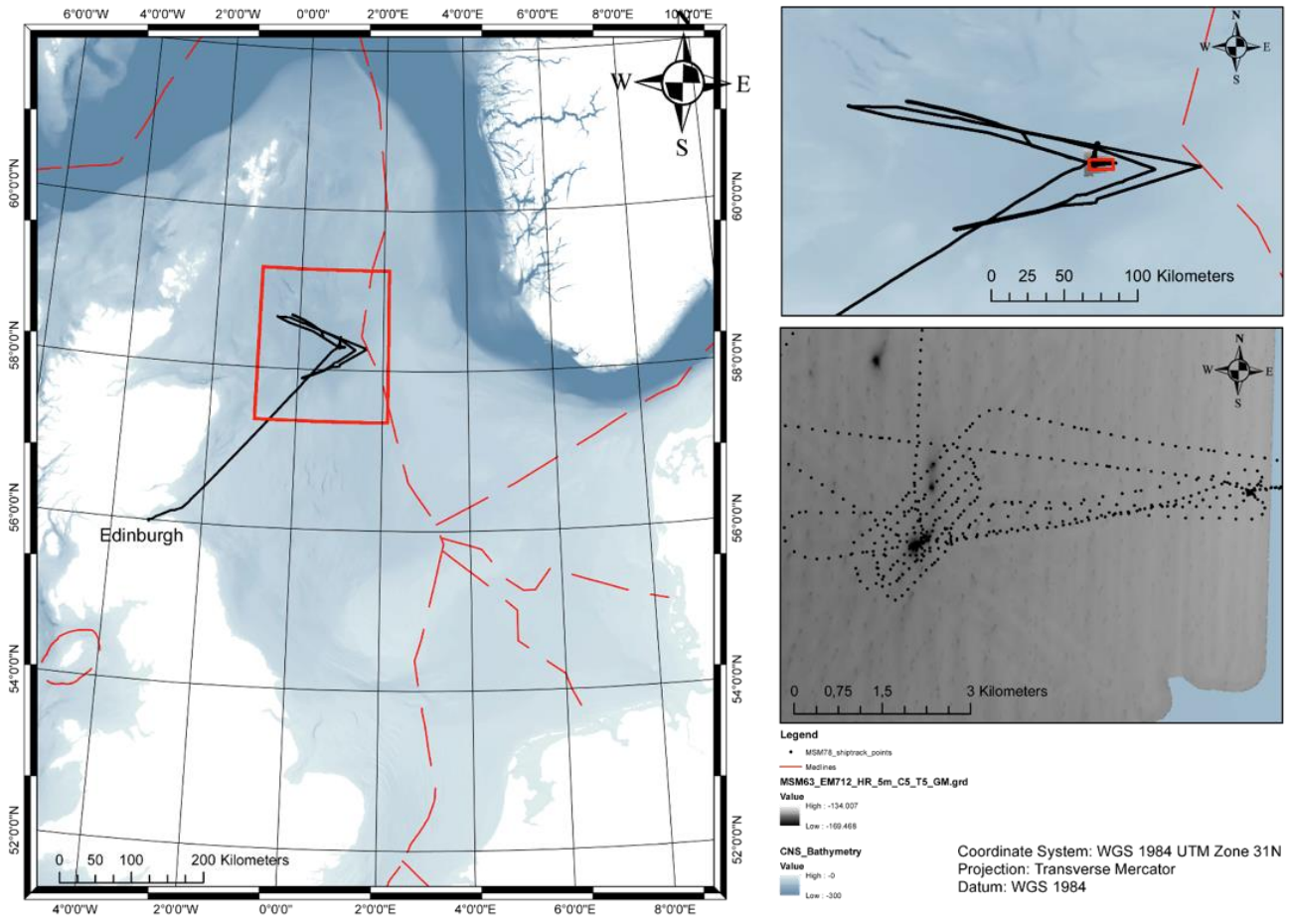

Figure 3: Cruise track of MSM78.

5 Preliminary Results

5.1 RockDrill2

5.1.1 Equipment and Method

The RockDrill2 (RD2) is a remotely operated multi-barrel wireline subsea robotic sampling system, capable of coring up to 55 m below the seafloor in water depths up to 4000 m. RD2 is about 4.75 m high and spans about 3.1 m at the extremities of its legs weighing 6000 kg in air and 5000 kg in water (Figure 4). RD2 can operate in water depth of up to 4000 m and can drill up to 55 m below seafloor (mbsf). The cores have a diameter of 61.1 mm. The system is launched from its own Launch and Recovery System (LARS), and it can continuously core in 1.72 m sections. RD2 also has the capability to deploy downhole measurement and monitoring equipment, including downhole logging tools and packer and plug systems.

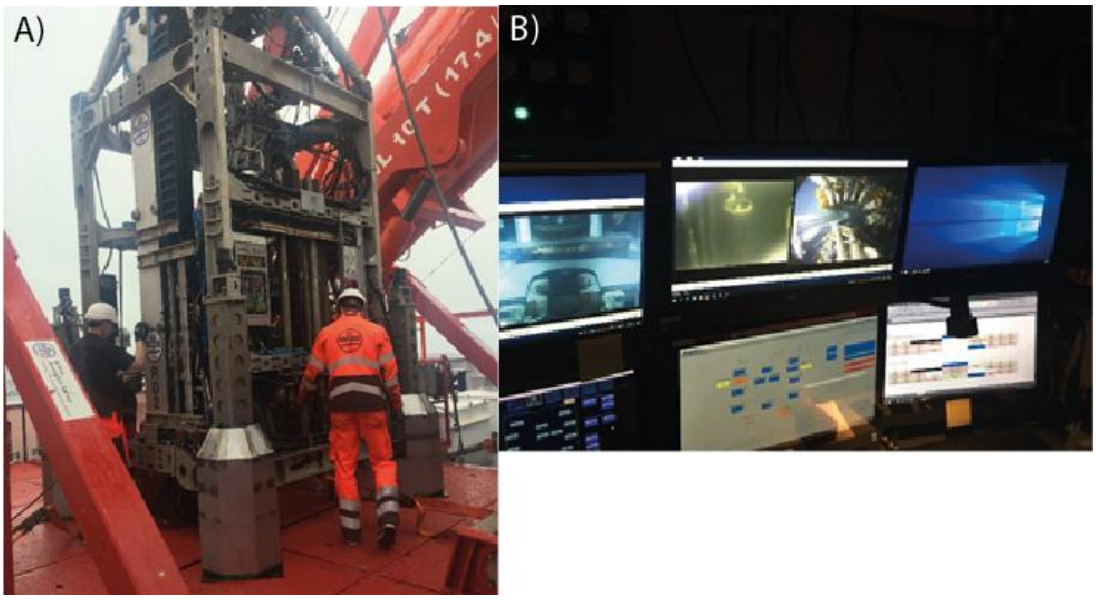

Figure 4: Rockdrill2 in operation during MSM78.A) RockDrill2 on board. B) Drilling operation in the control container.

The RD2 has coring capabilities for taking samples in various types of strata ranging from very hard lithologies such as gabbro, basalts and dolomites, to softer lithologies such as chalk and limestone and softer sediments such as marine and glacigenic sediments. The corer is remotely controlled from the surface via a combined fiber optic, power and lift cable. Continuous 1.72-meter core samples are taken using an internal core barrel, which is recovered through the main drill string with a wireline system. Core is then stored in the drill tool rack, subsea, until the target depth has been achieved. Prior to recovery, continuous in situ down-hole logging can also be carried out after coring operations are complete. On recovery to deck, all core samples are discharged. The stability of the drill on soft seabed sediments can be improved by means of extendable feet. These have been designed to be extended to preload the seafloor and allow vertical alignment of the drill to achieve optimal drilling orientation. The system has operated on unconsolidated seabed with a shear strength as low as 5 kPa. The RD2 can be outfitted with additional subsystem sensor packages such as CTD and Tracer injection. The borehole can be logged by a range of downhole logging tools. The BGS have an Optical, Acoustic and spectral Gamma (OAG) memory tool, dual-induction tool and magnetic susceptibility tool. A borehole plug can

also be installed in the cored hole. This isolates the borehole from the surrounding seafloor and seawater, allowing subsequent borehole waters sampling to be carried out by an ROV.

5.1.2 RockDrill2 operation summary

17/10/2018: The vessel arrived on site, and carried out a Multibeam survey of reference site and pockmark survey areas. The RD2 was prepared for a Wet Test that commenced at 17:00, on successful conclusion of the test the RD2 recovered to deck at 17:45. The RD2 then underwent a visual check and the Bottom Hole Assembly (BHA) was installed. The RD2 was deployed on to the test hole/ reference hole at 20:22 with the initial aim of coring two core runs totaling 3.44 meters, this was revised to 10 meters by the Principle Investigator (PI) and science party. Spud in drill string commenced at 21:23 and core operations continued to the end of day. Coring depth at start of day: 0 mbsf. Coring depth at end of day: 3.44 mbsf

18/10/2018: Coring operation continue for the next 24hrs, science meeting held to discuss coring strategy. Plan to core to 07:00 on the 19th to allow bad weather to pass. The coring was progressing well, with no coring or technical issues arising. Coring depth at start of day: 3.44 mbsf. Coring depth at end of day: 20.69 mbsf

19/10/2018: The Science meeting was held at 07:00, Coring depth was at 24mbsf. The decision made to finish core run and recover drill to move to the pockmark site. Final core depth 24:141mbsf. The RD2 was recovered to deck at 11:04, the Vessel moved to carry out survey and SVP for pockmark site. The RD2 was reset of deployment at Scanner Pockmark site during this survey, with it being ready at 16:30. The coring plan was to core in two core barrels to test core catcher performance on the pockmark site before committing to a coring run to the full target depth. On completion, the RD2 was recovered to deck at 20:00 and the core was inspected. The total penetration at this site was 3.45 mbsf with a core recovery average of 42.4%. The vessel position was adjusted as directed by the science plan to better position RD2 within the pockmark. During the setup of the RD2 and down hole logging tool for dive number 3 a small oil leak was detected on a valve pack oil compensator, this compensator was replaced and the RD2 was deployed at 23:30. During this deployment, a water leak detector within a Hi-flow valve pack triggered, necessitating the recovery of the RD2 to deck for inspection. The RD2 was on deck at 00:00.

20/10/2018: The RD2 was on deck at the 00:00 undergoing inspection and fault finding for a water detect alarm, the fault was traced to the link connector between the Hi-flow valve pack and its controller pack. The RD2 was deployed at 02:32 and on seabed at site 3 at 03:18 on conclusion of systems checks in the water column. Coring commenced at 03:58 and continued to 16:18, with a total coring depth of 11.60 mbsf. The RD2 was then setup for deployment on the Downhole Optical Acoustic and Gamma (OAG) logging tool. The tool was deployed to a hole depth of 9.34mbsf at 17:43 and logging of the borehole during recover of the string into the RD2. The logging tool suffered a unexpected activation delay and started logging at 18:11 which was a hole depths of 4.11mbsf. The RD2 completed this operation at 18:24 and the system was recovered to deck, on deck at 19:05. Between 19:05 and 22:25 the coring and logging tool were discharged from the RD2 and it was setup for the fourth sampling site, this would be the final planned site due to weather conditions. The science plan for site 4 was to return to Reference Site and open hole drill to 32mbsf on completion of that take 2 to 3 core samples depending on time and deploy the Magnetic Susceptibility downhole logging tool. The RD2 was deployed at 22:25 and was on seabed at 22:37. The open hole drill commenced at 22:44 and was at a depth of 7.425mbsf by the end of the day.

21/10/2018: The open hole operation continued until 04:53 when a depth of 32.0mbsf was reached, the RD2 was them reconfigured for coring operation with the removal of the open hole tool and the

deployment of a core barrel. Coring operation commenced at 06:22 at a depth of 32mbsf, two core runs were successfully completed by 10:29 to a coring depth of 35.44 mbsf. With the available operation weather window running out, one further core run with downhole logging was planned. Unfortunately, this was not achieved due to a bearing failure in the top drive that made it unsafe to continue. The drill string was then recovered into RD2 by 19:20 and the system was recovered to deck by 19:35. All samples were discharged from the system by 20:23.

5.1.3 Preliminary results of RockDrill2 operations during MSM78

During MSM78, the RockDrill2 was used during four dives and collected sediment samples at two study sites within and outside the Scanner Pockmark (Figure 5; Table 1).

Table 1: RockDrill2 operations during MSM78.

Dive	Dive 1 – MSM78-06	Dive 2 – MSM78-08	Dive 3	Dive 4 – MSM78-10	Dive 5 – MSM78-11
Date	17/10/2018	19/10/2018	19/10/2018	20/10/2018	20/10/2018
Location	Reference Site	Scanner Pockmark	No landing	Scanner Pockmark	Reference Site
Latitude	58° 0.291283'N	58° 0.28164'N		58° 281671'N	58° 0.291313'N
Longitude	1° 0.067583'E	0° 0.970624'E		0° 0.970681'E	1° 0.067602'E
Water depth	149 m	170 m	170 m	160 m	160 m
Penetration into sediments	24.14 m	3.45 m		11.1 m	35.4 m; first 32 m open hole
Logging tool	none	none		Optical Acoustic and Gamma	magnetic susceptibility (failed)
Core recovery	70 % Average	42 % Average		54 % Average	30 % Average

On recovery of the RD2 core liners from the drill barrels by the BGS team, the plastic liners were cleaned one by one, capped with end caps (yellow at the top/black at the bottom) and the barrel number, the core and section numbers and the orientation of the core (arrow pointing towards the sediment surface) was marked on the liner. Afterwards core recovery from each section was determined and drill cores were described as good as possible through the clear core liners (Figure 5). For the 1.7 m long RD2 liners, the parts that were filled with sediments were cut into smaller sections so that the sediments could not move inside the liners. Note that it is not possible to determine from where in the 1.7 m liner the sediment originates. Hence for operational reasons (e.g. subsampling), the upper part of the liner was considered to be filled with sediment and the lower part was considered to be lost. In some cases the cores were split into 2 subsection, labeled A (upper section) and B (lower section) – see Table 2 - 5. TheRD2 cores were not split onboard and were stored at 4 °C in the cold room of the Maria S. Merian for the duration of the cruise.

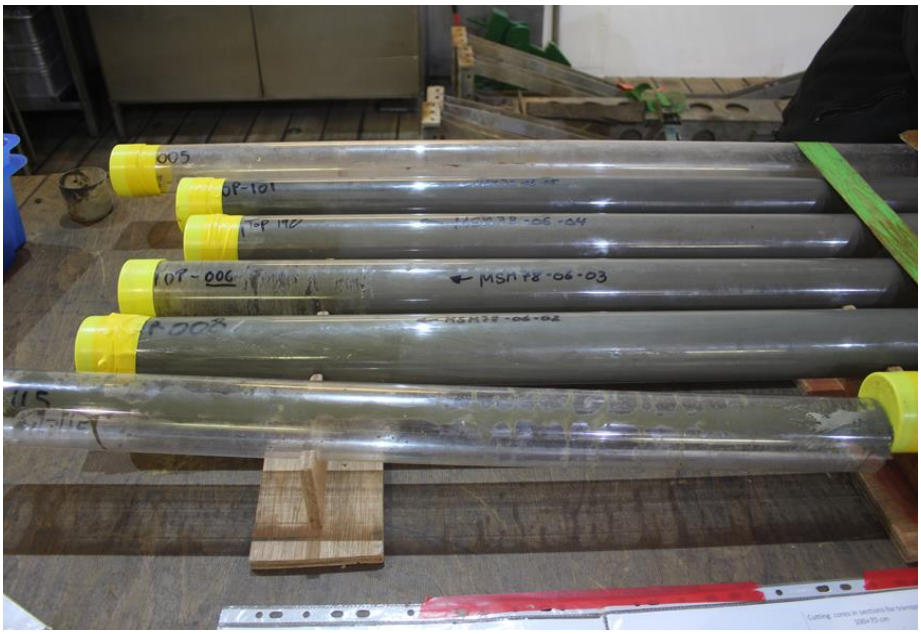

Figure 5: RockDrill2 core MSM78-06 collected at a reference site outside the Scanner Pockmark

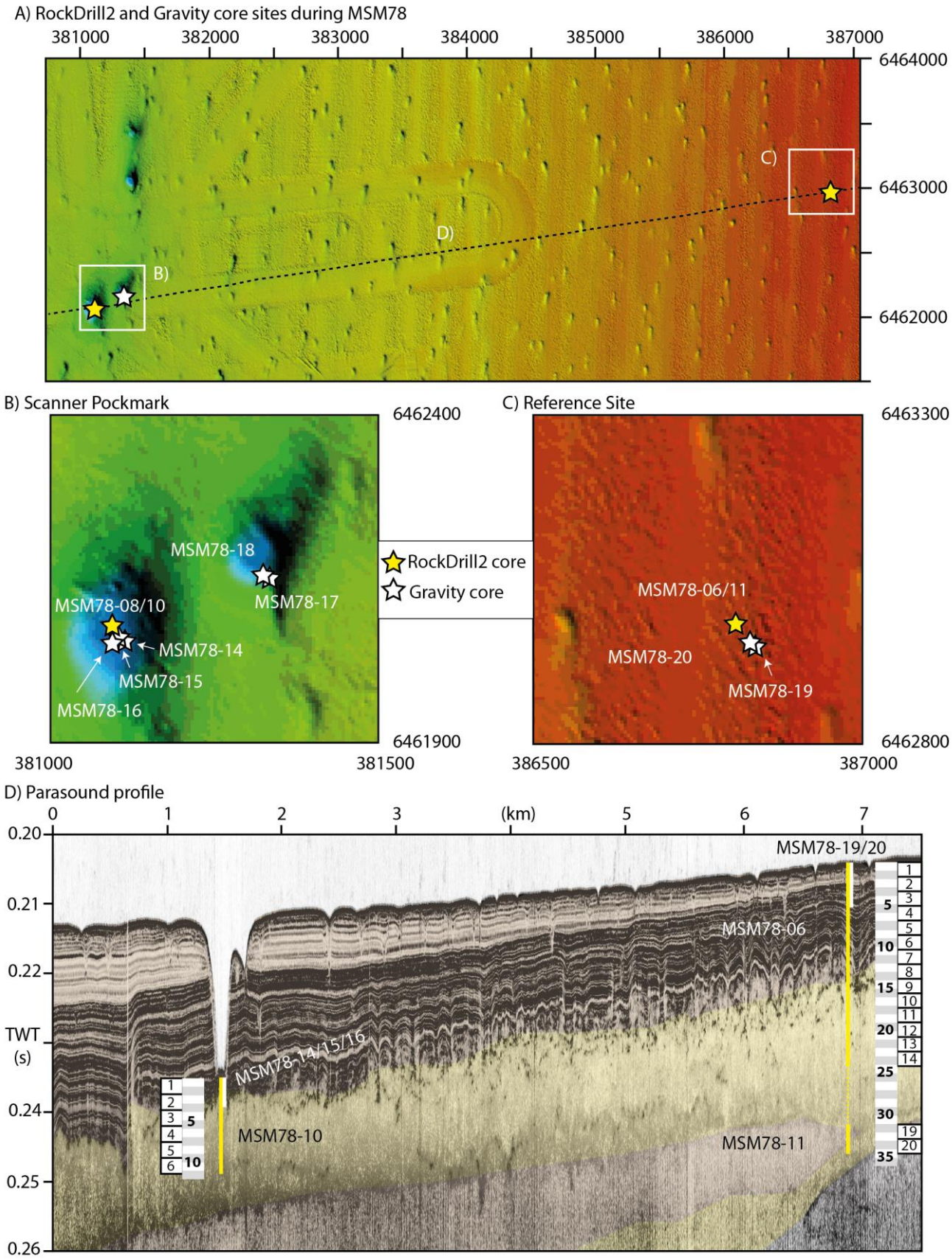

Figure 6: RockDrill2 and Gravity core sites during MSM78_ Overview map. B) Scanner Pockmark site. C) Reference site. D) Parasound profile crossing both drill sites.

Table 2 - 5 contains details and a short description of the 4 recovered RD2 cores. The sections are labeled: cruise number - station number - section number. The core sections increase in number below the sediment surface, such that Section 1 represents the section taken from closest to the sediment surface. In case there are Sections A and B, then A represents the upper part of the section and B the lower part of the section. The barrel number relates to the RD2 core barrel; cc= core catcher; cc and barrel together are 171.5 cm long. Note that sediment description, core length, % recovery are preliminary results and the tables will be updated after the cores have been split open in the onshore laboratories.

5.1.3.1 Dive 1 – bore hole 1: MSM78-06

Table 2: Core description MSM78-06

Section	Barrel no	Section Length (cm) (liner length: 166.5 cm)	Core catcher (cm)	% recovery without cc	% recovery with cc	Descriptions and comments
MSM78-06-1	115	86	3	51	52	Brown-greyish mud, homogenous, with darker brown smears
MSM78-06-2 (A/B)	008	167 (A=88 cm; B=79 cm)	8	100	102	Brown mud, disturbances from drilling visible between sediment and liner, full recovery
MSM78-06-3	006	142	2	85	84	Brown mud, homogenous
MSM78-06-4 (A/B)	091	163 (A=94 cm; B=69 cm)	1	98	96	Dark brown, full recovery
MSM78-06-5 (A/B)	101	168 (A=92 cm; B=76 cm)	9	101	103	Dark brown mud, sulfide smell, some back smears, full recovery
MSM78-06-6	005	43	8	26	30	Detached from the rest, 3-24 cm: disturbed from drilling, darker brown sediment
MSM78-06-7	131	105	7	63	65	Brown-greyish mud, homogenous, with darker brown smears
MSM78-06-8	009	56	9	34	38	Top very disturbed: with water running down the side of the liner at 15-25 cm
MSM78-06-9	119	108	5	65	66	Very disturbed on one side, vertical smears
MSM78-06-10	007	40	8	24	28	Very disturbed
MSM78-06-11	094	33	9	20	24	Very disturbed, different liner length
MSM78-06-12	067	59	10	35	40	Very disturbed
MSM78-06-13	003	107	12	64	69	Grey mud, darker than previously, black parts
MSM78-06-14 (A/B)	106	98 (A= 25cm; B=73 cm)	4	59	59	Many darker smears, Section A for permeability measurements (GEOMAR)

5.1.3.2 Dive 2 – bore hole 2:MSM78-08

Table 3: Core description of MSM78-08

Section	Barrel no	Section Length (cm) (liner length: 166.5 cm)	Core catcher, (cm)	% recovery without cc	% recovery with cc	Comment
MSM78-08-1	094	30	3	18	19	Homogenous grey mud, 4/1 5Y
MSM78-08-2	005	105	8	63	66	Greyish mud, homogenous, sulfidic smell, shell fragments in the upper part of the section, 3/10G Grey 2 (soil color scale)

5.1.3.3 Dive 4 – bore hole 3:MSM78-10

Table 4: Core description of MSM78-10

Section	Barrel no	Section Length (cm) (liner length: 166.5 cm)	Core catcher (cm)	% recovery without cc	% recovery with cc	Comment
MSM78-10-1	101	52	3	31	32	Some disturbances, greenish-yellow-grey:4/1 5Y to 4/2 5Y
MSM78-10-2	119	136	6	82	83	4 5B Gley 2, upper 30 cm light brown grey undisturbed, below grey with sub horizontal cracks
MSM78-10-3	131	0	5	0	3	Only cc recovered, here sediment very disturbed
MSM78-10-4 (A/B)	008	148 (A=82cm; B=66 cm)	6	89	90	4/1 to 571 5Y grey to greenish grey, upper 38 cm highly disturbed and cracks without orientation, next 38 cm more smooth less cracked, next 50 cm little disturbed, basal part smooth
MSM78-10-5	005	61	7	37	40	Section for SOTON (no subsampling)
MSM78-10-6 (A/B)	006	130 (A=25cm; B=105 cm)	4	78	78	4/1 to 5/1 grey to greyish, upper 25 cm (Section A) for GEOMAR , sample depth measured from top of section including section for GEOMAR, whole section slightly disturbed and with cracks of no orientation

5.1.3.3 Dive 5 – bore hole 4: MSM78-11

Table 5: Core description of MSM78-11

Section	Barrel no	Section Length (cm) (liner length:166.5 cm)	Core catcher (cm)	% recovery without cc	% recovery with cc	Comment
MSM78-11-19 (A/B)	106	46 (A = 31 cm; B= 15 cm)	8	9	13	3 samples from core catcher, pots 758 (porosity), 734 (freeze for Sr isotopes), 676 (frozen for redox sensitive sediments), + kept Section B intact for SOTON and GEOMAR
MSM78-11-20	091	45	8	27	31	Samples from core catcher, pots 696 (porosity), 695 (freeze for Sr isotopes), 684 pots 686,685 and 677 and RNA later with carbonate samples (frozen for redox sensitive sediments)

5.2 Gravity coring

During research cruise MSM78, we collected seven gravity cores within and outside the Scanner Pockmark (Figures 6 and 7; Table 6). All deployments were successful and recovered 29.5 m of core in total.

5.2.1 Equipment and Method

The GEOMAR gravity corer was fitted with a core barrel of 5.75 m length, a head weight of about 1.2 tons and a core catcher. Core liner, composed of opaque PVC-tubes of 5 m length and 12.5 cm diameter, are joined with pipe coupling pieces of 20 cm length. On R/V MARIA S. MERIAN, the gravity corer was deployed along the starboard side of the vessel, with an 18 mm steel cable attached to the ship´s winch. It was lowered with a rope speed of 0.5 m/s to the seafloor. Contact with the seafloor was monitored via the cable tension. The device remained on the seafloor for about 30 seconds in order to allow for deep penetration, and was then pulled out with a speed of 0.1 m/s. Heave velocity was 0.5 m/s.

After recovery and lashing of the gravity corer on deck, the core catcher was taken off and the liner pulled out of the core barrel. The core liner was oriented, labeled and cut into 1 m sections, whereas the deepest section was labeled as section 1. The top and base of each section is marked with "Top" and “Bottom", respectively, as well as with core number and section number (e.g. MSM78-18 section 2). Orientation arrows have the arrowheads pointing upward. The core was not split onboard. Three cores (MSM78-14, -16, -18) were selected for pore water analysis and sediment sampling, which requires holes of 5 to 10 mm drilled into the plastic liner. The cores were stored at 4°C. Cores from Station MSM78-15, -17 and -19 were sectioned and stored at 4 °C, but otherwise unprocessed for assessment of physical properties back in the laboratory in Southampton and Kiel.

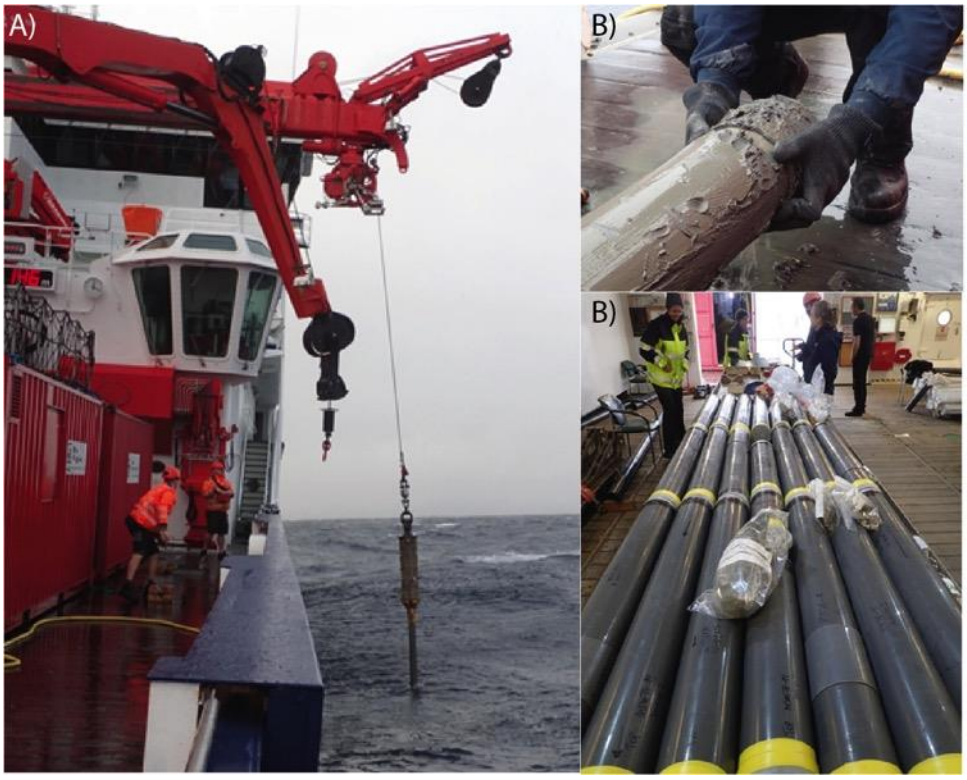

Figure 7: A) Gravity core before recovery. B) Opening of gravity core. C) Gravity core section in the wet lab.

5.1.2 Gravity cores

During MSM78, we collected seven gravity cores within and outside the Scanner Pockmark (Figure 6; Table 6).

Table 6: List of gravity cores obtained during MSM78

Station	Latitude (N)	Longitude (E)	Site	Water depth (m)	Total length of core recovered (m)	# of sections	Maximal penetration depth (mbsf)
MSM78-14	58°16.889	0°58.255	Scanner pockmark, site south 1	170	3.5	4	5.7
MSM78-15	58°16.888	0°58.258	Scanner pockmark, site south 1	168	3.3	4	5.7
MSM78-16	58°16.886	0°58.243	Scanner pockmark, site south 2	169	3.2	4	5.7
MSM78-17	58°16.944	0°58.476	Scanner pockmark, site northeast	165	4.5	5	5.7
MSM78-18	58°16.944	0°58.478	Scanner pockmark, site northeast	164	4.8	5	5.7
MSM78-19	58°17.463	1°04.080	Reference site	148	~5	6	5.7
MSM78-20	58°17.465	1°04.071	Reference site	148	5.3	6	5.7

5.3 Sediment geochemistry

5.3.1 Background

The geochemistry work during cruise MSM78 had three main objectives:

1) To characterize the chemical composition of fluids and gases migrating through the chimney: For this we collected pore water samples to determine species that influence reactions with leaking CO_2, including the carbonate system (dissolved inorganic carbon (DIC), total alkalinity (TA) and pH) and potentially harmful metals that may be released into the overlying water column, and species that trace fluid origin (e.g. $^{87}Sr/^{86}Sr$, Cl). These data will be used to parameterize reactive transport modelling that will be done by other work packages in the STEMM-CCS and CHIMNEY projects.

2) To determine the relationship between these parameters and permeability we will characterize core geology, including lithology, grain size distribution, sediment texture and porosity.

3) When split, we will recover samples of authigenic carbonates from the cores that then can be dated to ascertain the longevity of fluid flow.

Pore water and sediment samples were sampled from GC and RD2 cores (Appendix C). The scientific analyses required for these objectives cannot be conducted onboard, but require the collection of pore samples shortly after the recovery of the sediment cores.

5.3.2 Pore water sampling

For geochemical analyses, pore waters and sediment samples were extracted through small holes drilled into the liner of the RD2 and GC liners from Stations MSM78-14, -16, -18, -20. Porewaters were collected with Rhizones (0.2 µm pore diameter, type: CSS: length 5 cm for gravity cores and 2 cm for RD2 cores, Rhizosphere Research Products, Wageningen, Netherlands, Figure 8) approximately every 30 cm (see Appendix C). Solid phase samples were collected with cut-off 5 cm syringes.

Figure 8: Porewater subsampling from gravity cores with Rhizones.

Details of the methods for collection of sediments and pore waters are listed in, respectively, Tables 11 and 12, together with details of sample preservation. No on-board analyses were carried out and analyses of pore water and sediments will be performed in Southampton. Logs showing samples taken can be found in Appendix C.

Table 11: Sampling and preservation of sediments

Sampling Priority	**Sample Type**	**Volume of sediment**	**Preservation**
1	Hydrocarbon gases, CH_4 & C2-C6, isotopes and concentrations	3 cm^3	Crimp sealed in 5 mL 1M NaOH solution. Stored upside down at room temperature
2	RNA analysis	5 cm^3	Stored at 4 °C in 5 mL RNA later
4	DNA analysis	1 cm^3	Frozen at < -20°C
5	pH	Insert probe into porosity sample	On-board analysis with regular lab pH probe (Mettler Toledo)
6	Porosity and grain size analysis	3 cm^3	Stored at 4 °C in pre-weighed pot
7	Redox-sensitive metals	3 cm^3	Frozen at -20 °C in plastic bag
8	PFCs	1–5 cm^3	Stored at room temperature in 20 mL headspace vials with 5 mL MQ water

Table 12: Sampling and preservation of sediment pore waters.

Sampling Priority	Sample Type	Total Volume	Container - Preservative
1	Cations & Sr isotopes	2 mL	Stored in acid-washed LDPE bottle and with 10µL of sub-boiled HNO_3 added
2	Anions + H_2S	1 mL	Stored in pre-weighed LDPA vial containing 0.5 mL of 5% ZnAc
3	DIC	2 mL	Filled to brim and stored in glass screw cap vials. Poisoned with $HgCL_2$ and stored at 4°C
4	TA	2 mL	Filled to brim and stored in glass screw cap vials. Poisoned with $HgCL_2$ and stored at 4°C
5	$\delta^{18}O$, δD, $\delta^{13}C$-DIC	4.5 mL	Filled to brim and stored in glass screw cap vials. Poisoned with $HgCL_2$ and stored at 4°C
6	Nutrients	1 mL	Frozen at -20°C

5.3.3 Use of PFC tracer during ROCKDRILL2 operations

As RD2 utilises drilling fluid during coring operations, it is critical to assess whether any drill fluid has intruded into the cores, where it may contaminate the sediment pore waters. To this end, a Perfluorocarbon (PFC) tracer, Perfluoromethylcyclohexane, was deployed as part of RD2 operations (Table 13). Perfluorocarbons are widely used as tracers because they are non-toxic, unreactive, stable and can be detected even at very low concentrations ranges. Tracer preparation and sample handling followed Smith et al. (2000).

Table 13: Properties of the PFC tracer Perfluoromethylcyclohexane (Sigma-Aldrich, Lot#: BCBT 1675, technical grade 90%) used on MSM78.

Molecular weight [g/mol]	350.05
Boiling point [˚C]	76
Density [g/mL]	1.76
Solubility [mg/L]	~1

The procedure used is as follows. First, an appropriate amount of the tracer was transferred into an infusion bag. To minimise contamination, this was done on the top deck of the ship, which is well ventilated and far away from the drill rig and labs. Those handling the tracer wore overalls and gloves, and were not the same people who were involved in subsequent sampling and processing of the core material. The infusion bag was then attached to the tracer injection system pumping system mounted on RD2. The tracer injection system contains a micro annular gear pump mzr-2542 integrated in the filter-pump-valve (F-P-V) functional module allowing for precise and reproducible dosing. The tracer injection rate was 0.15 mL min^{-1} and was adjusted to achieve a final PFC concentration of 1 mg/L in the drilling fluid.

After retrieval of the core barrels and liners, the drill fluid was collected to verify that the PFC injection into the drill fluid was successful. The drill fluid was sampled into 50 mL centrifuge tubes, then 5 mL of the drill fluid where pipetted into 20 mL-headspace vials filled with 5 mL of Milli-Q, crimp sealed and stored at room temperature. Sediment samples from the centre of the core were taken to check whether drill fluid had intruded into inner part of the core, i.e. were pore waters were sampled from. The sediment was sampled using cut-off syringes (3 cm^3). The sediment samples were transferred into 20 mL-headspace vials filled with 5 mL of Milli-Q, crimp sealed and stored at room temperature. The PFC tracer system was used for RD2 Stations MSM78-6 and MSM78-10. Analysis of the samples will be done back on shore.

5.3.4 Preliminary observations

No analyses were done onboard the ship. Briefly, sediment cores from the reference site were softer to sample than any of the pockmark cores. The smell of H_2S was noted in one interval in core MSM78-06. Recovery using RD2 varies between 24 and 100%; it is presumed that sandy intervals were lost during drilling operations. Disseminated carbonate (white granular grains that fizzed in dilute HNO_3) was discovered in the core catcher of RD Core MSM78-11-20 (see Fig. 9).

Figure 9: Disseminated carbonates from the core catcher of MSM78-11-20.

Cores recovered from within Scanner Pockmark smelt strongly of H_2S in the upper parts, and an interval of shell fragments was recovered in the upper ~3m. Cut ends of cores recovered from the northeastern segment of Scanner (that is believed to be currently more active) had pervasive black blebs (most likely pyrite) in the sediments. Carbonate 'pavement' was not captured in any of the cores, although it was observed at the surface at the pockmark site by cameras mounted on RD2.

5.3.5 Further analysis

On return to Southampton measurements of various geological, physical and geochemical parameters, including lithology, grain size distribution, sediment texture, porosity, permeability, magnetic susceptibility, and fluid, gas and solid phase geochemistry, will commence. The physical properties of the sediment, P-wave velocity, gamma density (bulk density), magnetic susceptibility and non-contact resistivity will be measured on the whole cores with an MSCL (Multi-Sensor Core Logger) at BOSCORF (British Ocean Sediment Core Research Facility) in Southampton. Afterwards, the cores will be split horizontally into a working and an archive half, the lithology will be described and high-resolution photographs will be taken. If required, further samples will be collected from the working half. The archive half of the cores will be used to determine the down-core geochemical composition with the ITRAX XRF core scanner at BOSCORF. The archive and working halves of the cores will be stored at BOSCORF. Porosity and permeability will be determined on undisturbed parts of cores by CT-scanning at GEOMAR and SOTON.

5.4 Multibeam bathymetry

5.4.1 Equipment and Method

RV MARIA S. MERIAN is equipped with two Kongsberg Maritime multibeam echosounder. The EM122 system operates at 12 kHz and covers water depths from 20 meters below the transducers up to full ocean depth; while the EM712 system offers three different frequency ranges (40-100 kHz, 50-100 kHz, 70-100 kHz) of signals for water depths ranging from 3 m below transducers to roughly 3500 m. Two different transmit pulses can be selected: a CW (Continuous Wave) or FM (Frequency Modulated) chirp. In case of the EM712, the latter is part of the full performance version that is installed on RV Maria S. Merian. The sounding mode can be either equidistant or equiangular, depending on operation preferences and requirements. Both systems can be operated in single-ping or dual-ping mode, where one beam is slightly tilted forward and the second ping slightly tilted towards the aft of the vessel. The whole beam can also be inclined towards the front of the back and the pitch of the vessel can be compensated dynamically. The EM122 system produces 432 beams covering a swath angle of up to 150° while the EM712 system produces 512 beams for a maximum swath angle of 140°. The latter offers a high-density beam-processing mode with up to 800 soundings per swath. The swath angle, however, can be reduced, if required.

The transducers of both multibeam echosounder systems of RV MARIA S. MERIAN are mounted in a so-called Mills cross array, where the transmit array is mounted along the length of the ship and the receive array is mounted across the ship. The system on RV MARIA S. MERIAN is of a 1° x 1° design. The EM712 system installed on RV MARIA S. MERIAN is of a 0.5° x 0.5° design, but transducers are much smaller.

The echo signals detected from the seafloor go through a transceiver unit (Kongsberg Seapath) into the data acquisition computer or operator station. In turn, the software that handles the whole data acquisition procedure is called Seafloor Information System (SIS). In order to determine the point on the seafloor, where the acoustic echo is coming from, information about the ship's position, movement and heading, as well as the sound velocity profile in the water column are required. Positioning is implemented onboard RV MARIA S. MERIAN with conventional GPS/GLONASS plus differential GPS (DGPS) by using either DGPS satellites or DGPS land stations resulting in quasi-permanent DGPS positioning of the vessel. These signals also go through the transceiver unit (Seapath) to the operator station. Ship's motion and heading are compensated within the Seapath and SIS by using a Kongsberg MRU 5+ motion sensor. Beamforming also requires sound speed data at the transducer head, which is available from a Valeport MODUS SVS sound velocity probe. This signal goes directly into the SIS operator station. Finally, a sound velocity profile for the entire water column can be obtained either from a sound velocity probe or from a CTD (conductivity, temperature and density) probe. The temperature (T), salinity (S) and pressure (p) data acquired by any CTD (conventional or mounted on the AUV) can be converted into sound speed by using a sound speed function C(S,T,p). During cruise MSM78, we used direct sound velocity measurements with a special profiler probe at the beginning, mid and end of the cruise and for different survey areas.

In addition to bathymetric information, both the EM122 and the EM712 system register the amplitude of each beam reflection as well as a sidescan signal for each beam (so-called snippets). Both systems also allow recording the entire water column. The amplitude signals correspond to the intensity of the echo received at each beam. It is registered as the logarithm of the ratio between the intensity of the received signal and the intensity of the output signal, which results in negative decibel values. For each ping, EM122 records 432 backscatter intensity values while the EM712 records 800 backscatter values. The water column data correspond to the intensity of the echoes recorded from the instant the output signal is produced. All echoes coming from the water column, the seabed and even below the seabed

are recorded for each beam. When the water column data of one ping is divided into a starboard and port subsets, one can produce two traces, one for each subset. Each trace is build up as a time series in which for each time the highest amplitude is selected from all beams. Then the starboard and the port traces are joint together.

5.4.2 Acquisition Parameters

During cruise MSM78, the Kongsberg EM122 system was not used, due to the low water depth in the central North Sea. Acquisition parameters for the EM712 system were set the following. The pulse was FM, ping mode was set to high-resolution equidistant, dual ping mode was switched off, and depth mode was set to automatic. The beam angle was reduced to 120° during most of the survey, except for the surveys, where the maximum coverage was desired. Survey speed varied between 5 and 8 knots. Data were acquired continuously during pre-designed surveys. A trigger box to organize the soundings of different systems is now present on RV MARIA S. MERIAN. Therefore, we could acquire data with the PARASOUND P70 and the EM712 without strong interferences. Unfortunately, due to unresolved problems, we faced very low ping rates of the EM712 of up to 10 s interval in between single pings. The trigger software showed that the EM712 was pinging correctly bus was "busy" for very long timescales storing and processing the data. This made an acquisition of water column data inefficient. Water column data were not recorded throughout the cruise due to these low pinging rates. SVP casts were conducted before, during and after the research program. The EM712 system was running stable throughout the cruise (Figure 10).

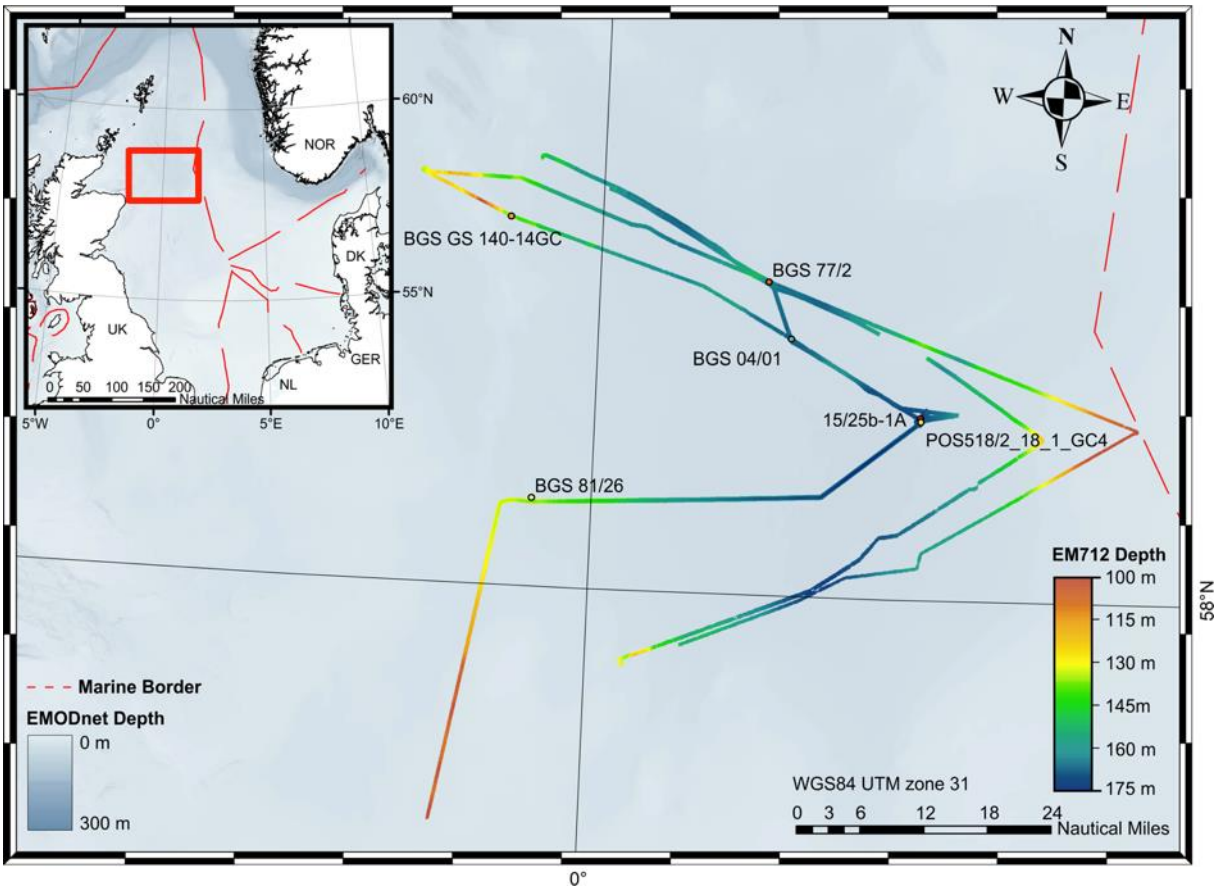

Figure 10: EMODnet bathymetry (blue colored) of the Witch Ground Basin, central North Sea, and acquired bathymetric data (multicolored). (INSET) Inset shows the location of the survey area (red box) within the North Sea. Dashed red line shows the political boundaries. The map shows numerous boreholes from the British Geological Survey (BGS), industry well 15/25b-1A and gravity core POS518/2_18_1_GC4 acquired during Poseidon cruise 518 leg 2.

5.4.3 Data Processing

Data processing has been carried out onboard using different software packages (MB Systems, QPS Fledermaus). Within MB Systems Version 5.5.2303 (release: April 28, 2017) the processing and gridding of EM712 data took place. The soundings were preprocessed from Kongsberg all-format to an internal MB Systems format (format: 59).

The pings were cleaned in two steps (mbareaclean, mbclean). First we applied an area-filter with 15 m bin size, which flags all bad soundings with more than one standard deviation from surrounding (N=10 pings). Furthermore, we flagged all soundings with a deviation of 2% from the local (N=10 pings) median. Second, we applied a swath-filter, which flags 20 outer beams (highly influenced by noise), zaps bad rails (10 m) and cleans all pings outside 10% of the mean depth for each swath. Residual bad soundings or spikes were cleaned with the manual 3D ping tool (mbeditviz). The survey area is impacted by tides with ±0.5 m. Therefore, the OTPS model TPX-O8-Atlas v1 (resolution 1/30°) was used to calculate the tidal water level time series for correcting bathymetry (mbotps).

The data were subsequently gridded with MB-Systems using a Gaußian weighted mean with a cell size of 15 m. To eliminate unwanted influence of outer beams on the grid, induced by deviation of the outer beams, we applied a spline tension with a value of 2. All data were interpolated for a maximum of 3 cell sizes to achieve good coverage for the high-resolution grid

5.4.4 Backscatter

The backscatter (amplitude) signal is stored and preprocessed automatically by the Kongsberg software Seafloor Information System (SIS), including altitude processing, time varying gain (TVG) and angle varying gain (AVG). Backscatter data were processed onboard using FMGeocoder. The backscatter have been processed using FMGeocoder, where radiometric corrections, filtering, angle-varying gain and anti-aliasing filters are applied to the backscatter data before outputting a georeferenced mosaic.

5.4.5 Water column imaging

The EM712 multibeam echosounder produces a second type of raw data files with extension *.wcd, which stores water column data. These files were imported into QPS FMMidwater. The raw multibeam echosounder data (.all format) and associated water column data (.wcd) were placed into a single folder and imported into FMMidwater. Each line was subsequently opened in Swath Editor and displayed as a curtain image (along track, viewed from starboard side) and a time-series video (across track, viewed from stern). The data were also filtered by intensity. The .wcd format files showed a total record range of 1889.3 m, which might explain the long response time of the EM712 during acquisition (Figure 11). Due to the low ping rate we were not able to identify any features in the water column.

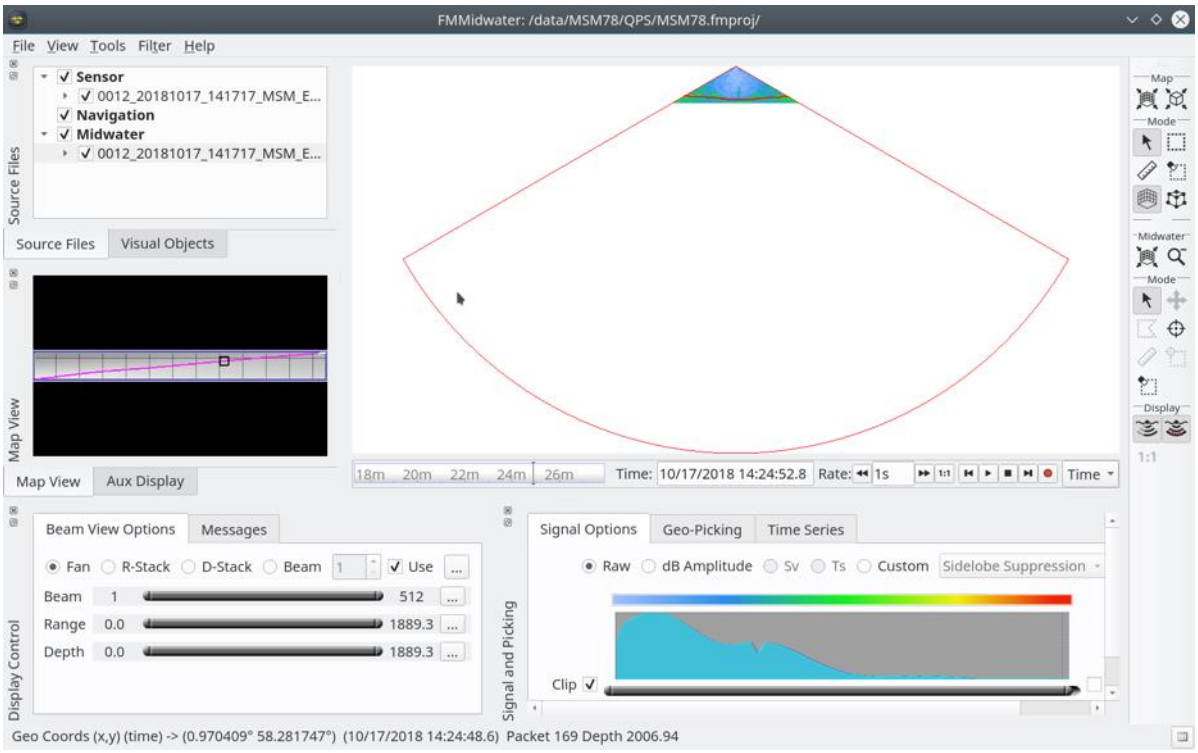

Figure 11: Processing of .wcd files with QPS FMMidwater shows the large record range, which might be inducing the long response and storage times of the EM712 during acquisition. During the cruise no solution for the problem could be identified.

5.4.6 Preliminary results

The bathymetric map of the Scanner Pockmark shows two clear depressions of the seafloor. The measurements show depressions of elliptical shape with 180 m diameter in North-South direction and 160 m in East-West direction. The depth is ~16 m in comparison to the surrounding seafloor. North of the Scanner pockmark, the Scotia pockmark is visible. Similar to the Scanner Pockmark this feature is an elliptical shaped. Both large sized pockmarks are surrounded by smaller sized depressions with tens of meters in diameter and only 1-3 m in depth. Few of these large-scale pockmarks exists, which have not been named before, indicating that these unusually large pockmarks are more frequent than previously proposed.

The Witch Ground Basin shows pockmarks of various sizes at the seafloor (Figure 12). One predominant group of pockmarks comprises pockmarks with tens of meters in diameter and 1-3 m in depth. These pockmarks occur where the Witch Ground Formation is present and are absent in areas where deposits of the last glacial maximum (LGM) crop out at the seafloor. The density and shape of these pockmarks changes with sediment thickness and location within the Witch Ground Basin indicating a strong dependency on the hosting sediments. The elongated shapes of the pockmarks show distinct strike directions, which may be attributed to local bottom currents reshaping the seafloor.

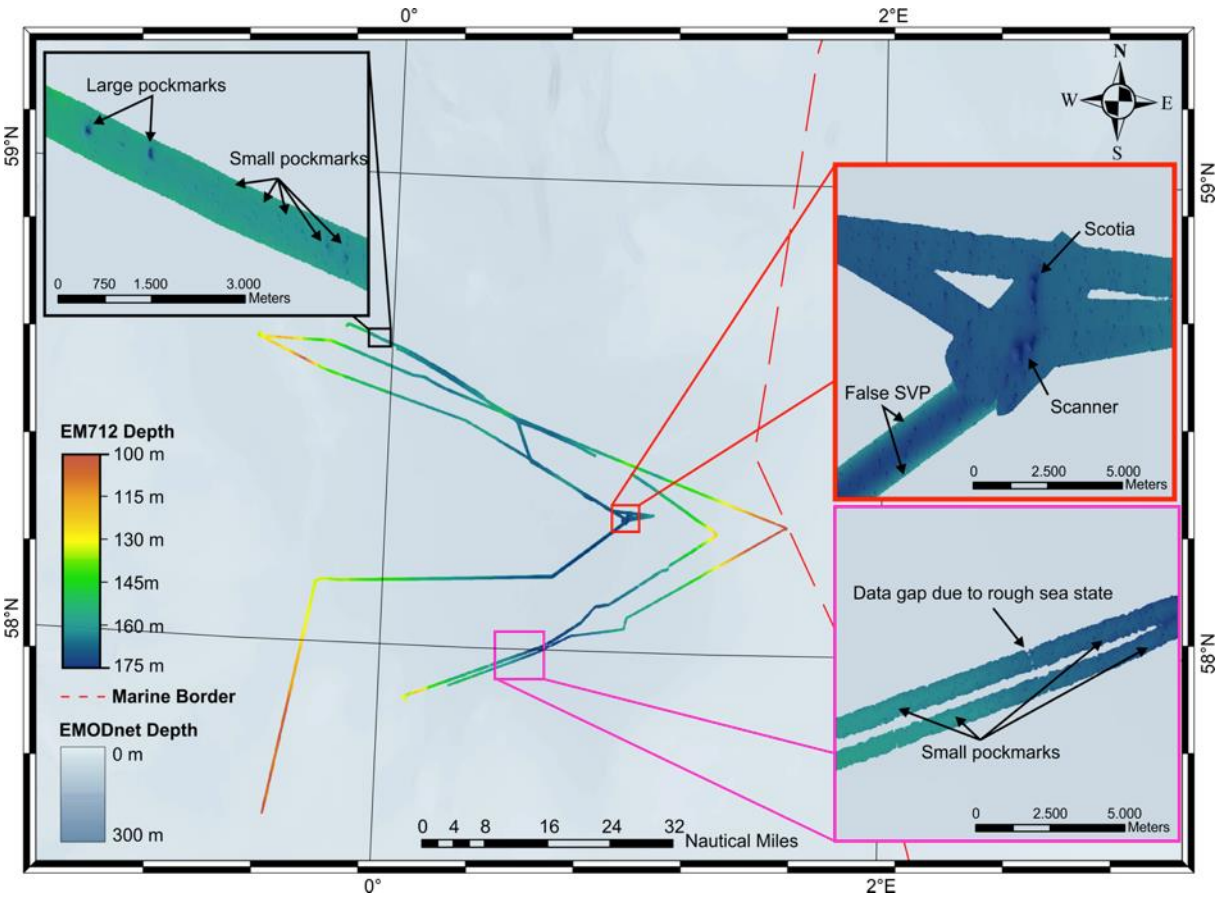

Figure 12: EMODnet bathymetry of the Witch Ground Basin and draped acquired EM712 bathymetry. The insets show prominent morphological features of the seafloor. (Black box) Unusually large pockmarks surrounded by smaller scale pockmarks in the northwestern part of the Witch Ground Basin. (Red box) The prominent Scanner and Scotia pockmark complexes comprising two large adjacent pockmarks. The bathymetry in the southwestern part shows upward bending of outer beams indicating an inappropriate sound velocity profile (SVP). (Pink box) Numerous small pockmarks with tens of meters in diameter and few meters depth. The rough sea state during acquisition induced major gaps in data where the EM712 failed to track the seafloor.

5.5 Parasound echosounder

5.5.1 Equipment and Method

The hull-mounted parametric sub-bottom profiler PARASOUND P70 (Atlas Hydrographic) was operated on a 24-hour schedule for flare imaging and to provide high-resolution (less than 15cm for sediment layers) information on the uppermost 50-100 m of sediment. The system has a depth range of 10 m to > 11000 m (full ocean depth) and a maximum penetration of 200 m. This high sediment penetration is acquired through the high pulse transmission power of 70 kW.

The RV Maria S. Merian is equipped with a PARASOUND P70 system since the start in 2007. PARASOUND P70 works as a narrow beam sediment echo sounder, providing primary frequencies of 18 (PHF) and adjustable 18.5 – 28 kHz, thus generating parametric secondary frequencies in the range of 0.5 – 6 kHz (SLF) and 36.5 – 48 kHz (SHF) respectively. The secondary frequencies develop through nonlinear acoustic interaction of the primary waves at high signal amplitudes. This interaction occurs in the emission cone of the high-frequency primary signals, which is limited to a beam width of 4.5° x 5°

for the PARASOUND P70. The system consists of four identical transducer modules, each about 0.3 m x 1.0 m. The P70 version includes 384 acoustic elements combined to form 128 stave channels. Therefore, the footprint size is approx. 4% of the water depth and vertical and lateral resolution is significantly improved compared to conventional 3.5 kHz echo sounder systems. The system provides features like recording of the 18 kHz primary signal and both secondary frequencies, continuous recording of the whole water column, beam steering, different types of source signals (continuous wave, chirp, barker coded) and signal shaping. Digitization takes place at 98 kHz to provide sufficient sampling rates for the high secondary frequency. A down-mixing algorithm in the frequency domain is used to reduce the amount of data and allow data distribution over Ethernet.

5.5.2 Acquisition Parameters

For the standard operation, a parametric frequency of 4 kHz (SLF) and a sinusoidal source wavelet of 3 periods were chosen to provide a good balance between signal penetration and vertical resolution. The 18 kHz signal (PHF) was also recorded permanently.

At the survey area, the system was mainly used for analysis of sedimentary processes, such as identification of different phases of glacial deposition or erosion. Due to low water depth (< 200m) at the survey area the PARASOUND system was operated in a single pulse mode.

The system worked reliable and produced high-quality data throughout the whole time (Figure 13). A trigger box to organize the signals of the EM712 and PARASOUND P70 during acquisition, reducing the ping rate but enabling simultaneous acquisition without major induced artifacts due to interference of both systems. The triggered signals worked well for the PARASOUND P70, but caused problems within the EM712 and water column imaging (see above).

All raw data were stored in the ASD data format (Atlas Hydrographic), which contains the data of the full water column of each ping as well as the full set of system parameters. Additionally a 200 m-long reception window centered on the seafloor was recorded in the compressed PS3 and SEGY data format after mixing the signal back to a final sampling rate of 12.1 kHz. This format is in wide usage in the PARASOUND user community and the limited reception window provides a detailed view on subbottom structures.

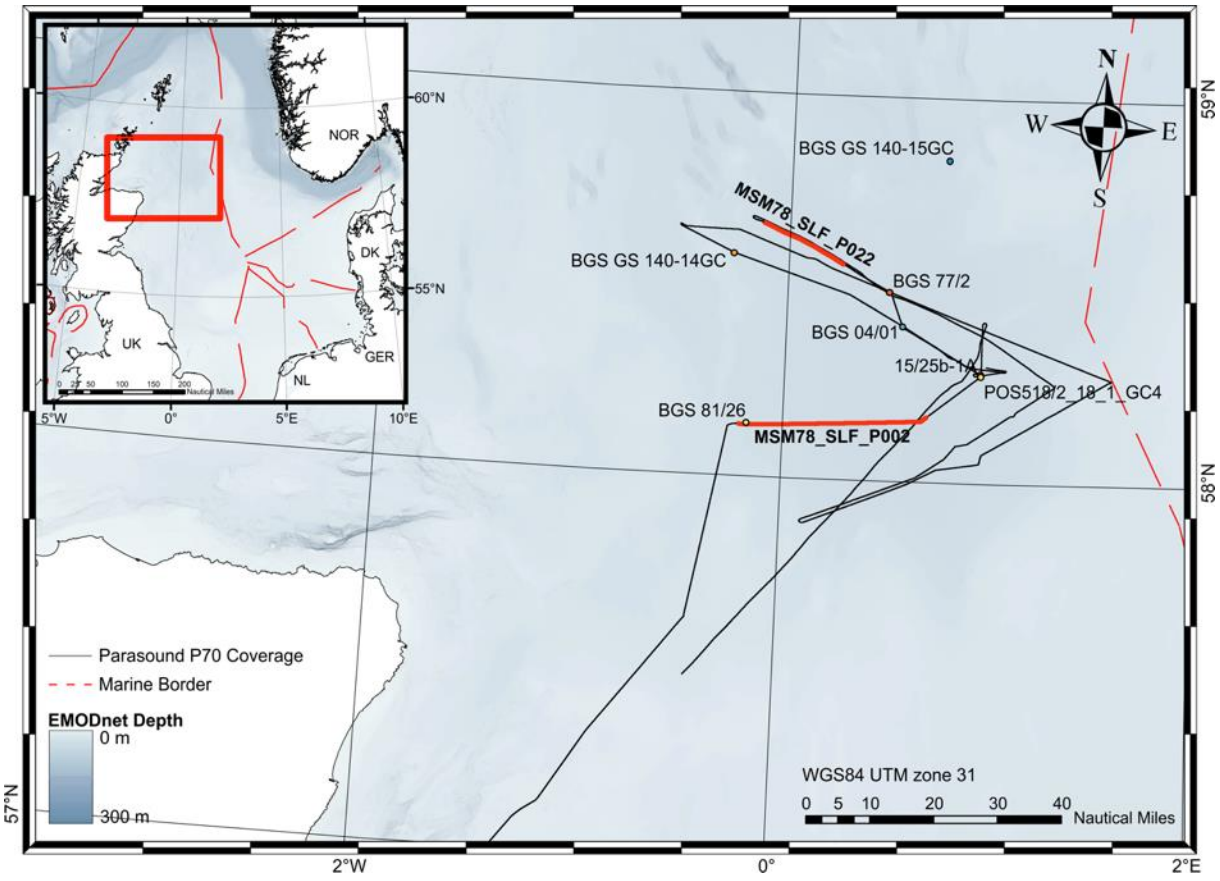

Figure 13: Overview of acquired PARASOUND P70 profiles. Red lines show location of profiles shown below. The map shows numerous boreholes from the British Geological Survey (BGS), industry well 15/25b-1A and gravity core POS518/2_18_1_GC4 acquired during Poseidon cruise 518 leg 2. In addition to the newly acquired sediment samples from the BGS RockDrill2, these sediment cores will be used to utilize a local to regional seismo-stratigraphic framework for the Witch Ground Basin.

5.5.3 Data Processing

All data were converted to SEG-Y format during the cruise using the software package ps32sgy (Hanno Keil, Uni Bremen). The software allows generation of one SEG-Y file for longer time periods, frequency filtering (low cut 2 kHz, high cut 6 kHz, 2 iterations), subtraction of mean and envelope calculation. We used the frequency filtering and loaded all data to the seismic interpretation software HIS Kingdom. The Envelope was calculated subsequently within the IHS Kingdom. One SEG-Y file was created for the length of each profile (Figure 13). In all other cases 2h-long pieces were generated (e.g. during transit, long seismic lines). This approach allowed us to obtain a first impression of sea floor morphology variations, sediment coverage, sedimentation patterns along the ship's track and imaging of glaciation phases. In addition, the data was converted from time to depth domain with an average velocity of 1500 m/s to select locations for the BGS RockDrill2.

5.5.4 Preliminary results

We used the PARASOUND P70 to analyze and interpret the uppermost sedimentary succession in the survey area, located in the central North Sea (Figure 13 & 14). Despite the expected coarse-grained material and glacial tills on the North Sea seafloor, the system showed very good penetration rates, in

some cases exceeding 60 m below the seafloor (Figure 14).

The overall penetration in the Witch Ground Basin was very good and in many parts up to 30 m into the subsurface. We used the very high-resolution PARASOUND P70 profiles in addition to the existing 3D seismic data, to verify previously proposed drilling targets for the BGS's RockDrill2. Furthermore, we used the PARASOUND P70 system to identify and verify any fluid conduits reaching to the surface. Due to the high-frequency signal, the system is highly sensitive to fluids or gases within the sedimentary succession and above the seafloor. This step was necessary especially for the proposed drilling targets to prohibit any unforeseen problems for the BGS's RockDrill2.

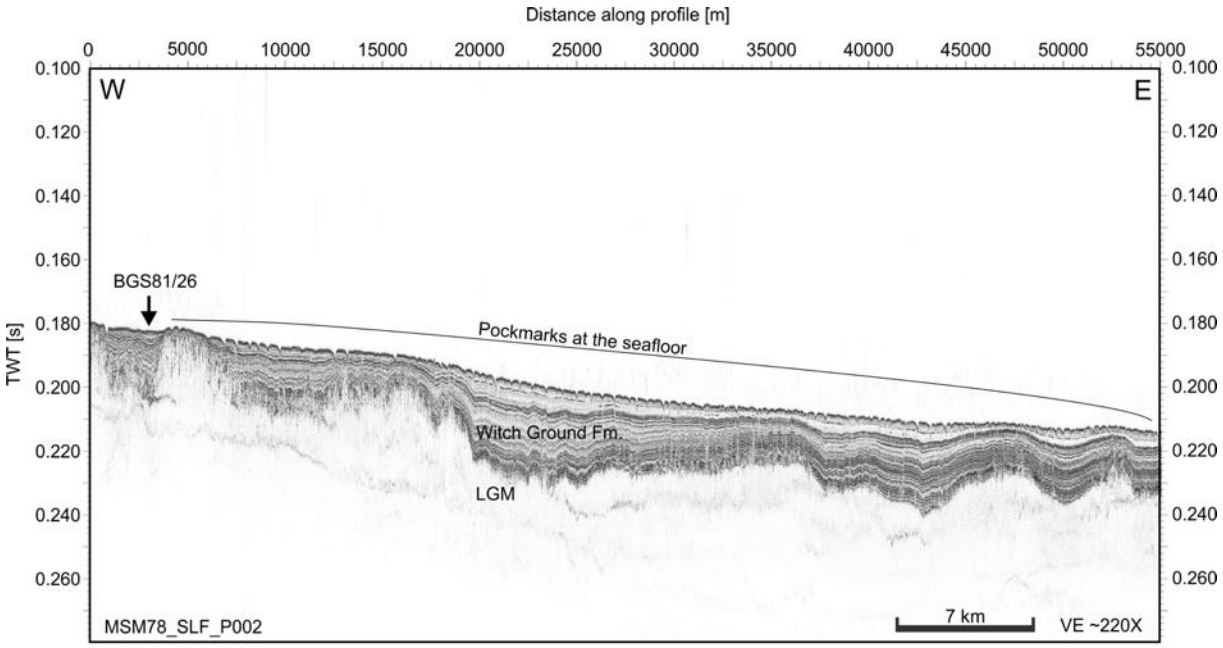

Figure 14: 55-km-long PARASOUND P70 profile acquired during MSM78 showing numerous pockmarks at the seafloor, the Witch Ground Formation and LGM deposits below. The location of borehole BGS81/26 is indicated with a black arrow. The y-axis is 220 times vertical exaggerated to the x-axis (at 1500 m/s sound velocity).

Regional profiles across the Witch Ground Basin (Figure 13) will help advance our understanding of sedimentary processes during and after the LGM (Figures 14 & 15). These profiles cross over a number of boreholes and will help tie our RockDrill2 results into a local and regional stratigraphic framework. Furthermore, we were able to trace the Witch Ground formation over a large area and identify geological features such as pockmarks, channels and fluid migration pathways. The high-resolution images show the numerous pockmarks at the seafloor within the Witch Ground Basin. These pockmarks are located in areas where the Witch Ground Formation is present.

The Coal Pit formation (below LGM) represents the acoustic basement for the PARASOUND P70 data. The LGM shows a highly corrugated surface with a number of tunnel valleys intersecting this stratigraphic unit. The seismic facies of these glacial deposits are transparent to chaotic and give insights on the poor sorting of the glacial tills. Small impedance contrasts in between each unit separate the different phases of sediment deposition and erosion. Steeply dipping reflections within these units indicate the presence of tunnel valleys (Figure 15).

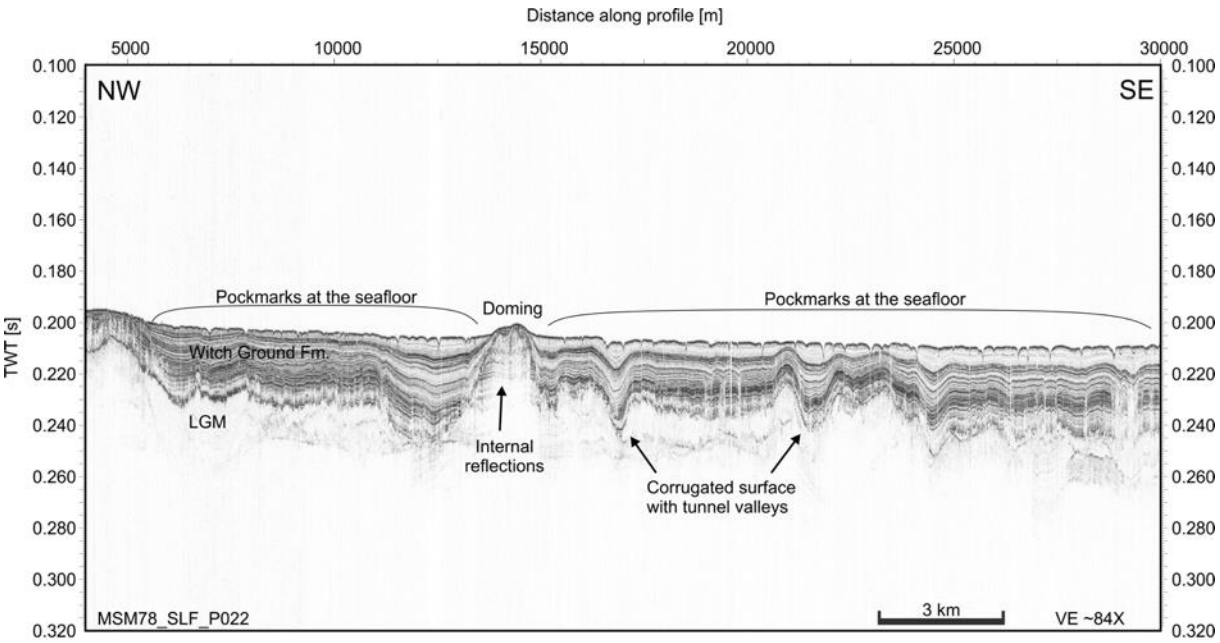

Figure 15: 30-km-long PARASOUND P70 profile acquired during MSM78 showing numerous pockmarks at the seafloor and possible sediment doming (onlap of surrounding sediments) with internal reflections. The imaged sedimentary succession comprises the Witch Ground Formation and LGM deposits below. The corrugated surface of LGM deposits indicates complex patterns of sediment erosion and deposition. The surface is intersected by numerous tunnel valleys or ice berg plough marks.

6. Acknowledgements

We would like to thank Captain Ralf Schmidt and the entire crew of R/V Maria S. Merian for their excellent support and hospitality during the entire cruise. Due to the professional guidance of the bridge and the crew, we could manage to acquire a maximum of sediment samples and geophysical data under challenging weather condition of the North Sea in late October. We would like to thank crew on deck, in the machine and the caboose for providing an encouraging and supportive working environment. This cruise was funded by EU within the framework of the Horizon 2020 initiative project STEMM-CCS und der grant agreement n°654462.

7. References

Andresen, K.J., 2012. Fluid flow features in hydrocarbon plumbing systems: What do they tell us about the basin evolution? Marine Geology 1–20. doi:10.1016/j.margeo.2012.07.006

Arntsen, B., Wensaas, L., Løseth, H., Hermanrud, C., 2007. Seismic modeling of gas chimneys. Geophysics 72, 251–259.Arts, R.J., Chadwick, R.A., Eiken, O., Thibeau, S., Nooner, S., Lamont-Dohery Geological Observatory of Columbia University, 2008. Ten years‘ experience of monitoring CO2 injection in the Utsira Sand at Sleipner, offshore Norway

Berndt, C., 2005, Focused fluid flow in passive continental margins: Philosophical Transactions of the Royal Society A, v. 363, S. 2855-2871.

Berndt, C., Elger, J., Böttner, C., Gehrmann, R., Karstens, J., Muff, S., Pitcairn, B., Schramm, B., Lichtschlag, A. and Völsch, A., eds., 2017. RV MARIA S. MERIAN Fahrtbericht / Cruise Report MSM63 - PERMO, Southampton – Southampton (U.K.) 29.04.-25.05.2017. Open Access . GEOMAR Report, N. Ser. 037 . GEOMAR Helmholtz-Zentrum für Ozeanforschung Kiel, Kiel, 137 pp. DOI 10.3289/GEOMAR_REP_NS_37_2017.

Bünz, S., Mienert, J., Berndt, C., 2003. Geological controls on the Storegga gas-hydrate system of the mid-Norwegian continental margin. Earth and Planetary Science Letters 209, 291–307. doi:10.1016/S0012-821X(03)00097-9

Cartwright, J.A., Huuse, M., Aplin, A., 2007. Seal bypass systems. Bulletin 91, 1141–1166. doi:10.1306/04090705181

Chadwick, R.A., Noy, D., Arts, R.J., Eiken, O., 2009. Latest time-lapse seismic data from Sleipner yield new insights into CO2 plume development. Energy Procedia 1, 2103–2110. doi:10.1016/j.egypro.2009.01.274

Exley, R. J. K., Westbrook, G. K., Haacke, R. R., & Peacock, S. (2010). Detection of seismic anisotropy using ocean bottom seismometers: a case study from the northern headwall of the Storegga Slide. Geophysical Journal International, 183(1), 188-210.

Gay, A., Mourgues, R., Berndt, C., Bureau, D., Planke, S., Laurent, D., Gautier, S., Lauer, C., Loggia, D., 2012. Anatomy of a fluid pipe in the Norway Basin: Initiation, propagation and 3D shape. Marine Geology 1–14.

Granli, J.R., Arntsen, B., Sollid, A., Hilde, E., 1999. Imaging through gas-filled sediments using marine shear-wave data. Geophysics 64, 668–677.

Gasda, S. E., Bachu, S., Celia, M.A., 2004 Spacial characterization of the location of potentially leaky wells penetrating a deep saline aquifer in a mature sedimentary basin. Environmental Geology 46, 707-720.

Gurevich, A. E., Endres, B. L., Robertson, J. O., & Chilingar, G. V. (1993). Gas migration from oil and gas fields and associated hazards. Journal of Petroleum Science and Engineering, 9(3), 223-238.

Heggland, R., 1998. Gas seepage as an indicator of deeper prospective reservoirs. A study based on exploration 3D seismic data. Marine and Petroleum Geology 15, 1–9.Hovland and Sommerville, 1985;

Judd, A., and Hovland, M., 2007, Seabed fluid flow: the impact on geology, biology and the marine

environment. Cambridge: Cambridge University Press.

Karstens, J. and Berndt, C. (2015) Seismic chimneys in the Southern Viking Graben – Implications for palaeo fluid migration and overpressure evolution. Earth and Planetary Science Letters, 412 . pp. 88-100. DOI 10.1016/j.epsl.2014.12.017.

Karstens, J. (2015) Focused fluid conduits in the Southern Viking Graben and their implications for the Sleipner CO2 storage project. (Doctoral thesis/PhD), Christian-Albrechts-Universität, Kiel, 183 pp.

Key, K., Constable, S., Matsuno, T., Evans, R.L. and Myer, D. (2012) Electromagnetic detection of plate hydration due to bending faults at the Middle America Trench Earth and Planetary Science Letters 351, 45-53.

Løseth, H., Gading, M., Wensaas, L., 2009. Hydrocarbon leakage interpreted on seismic data. Marine and Petroleum Geology 26, 1304–1319. doi:10.1016/j.marpetgeo.2008.09.008

Løseth, H., Wensaas, L., Arntsen, B., Hanken, N.-M., Basire, C., Graue, K., 2011. 1000 m long gas blow-out pipes. Marine and Petroleum Geology 28, 1047–1060.

Nicoll, D.G., 2011. Evaluation of the Nordland Group overburden as an effective seal for the Sleipner CO2 storage site (offshore Norway) using analytical and stochastic modelling techniques. PhD Thesis, School of Geosciences, University of Edinburgh, 383 pages

Smith, David C., et al., 2000."*Methods for quantifying potential microbial contamination during deep ocean coring*." Ocean Drilling Program Technical Note (2000).

Appendices

Appendix A: Station Book

Activity - Device Operation	Timestamp	Device	Action	Depth (m)	Speed (kn)	Course	Latitude (deg)	Longitude (deg)	Wind Dir	Wind Velocity	Winch	Rope Length (m)	Comment
MSM78_22-1	24.10.2018 14:24	Parasound	profile end	132.8	7	353	58.411.265	0.97076	281	37.4	ERROR	0	
MSM78_22-1	24.10.2018 12:50	Parasound	profile start	161	0	170	58.281.327	0.971076	288	31.4	EL1	0	rwk=000−
MSM78_21-1	24.10.2018 12:50	Sound Velocity Profiler	on deck	165.2	0	188	58.281.321	0.971079	288	31.4	EL1	-14	
MSM78_21-1	24.10.2018 12:43	Sound Velocity Profiler	max depth/on ground	162.5	0	21	58.281.346	0.971063	292	33.6	EL1	160	
MSM78_21-1	24.10.2018 12:37	Sound Velocity Profiler	in the water	161	0	75	58.281.352	0.971049	287	37.3	EL1	0	
MSM78_20-1	24.10.2018 11:32	Gravity corer	on deck	148.2	1	65	5.829.106	1.068	286	31. Jan	F1S1	-9	
MSM78_20-1	24.10.2018 11:23	Gravity corer	max depth/on ground	148.9	0	143	58.291.083	1.067.842	286	26. Sep	F1S1	147	
MSM78_20-1	24.10.2018 11:19	Gravity corer	in the water	146.7	0	15	58.291.048	1.067.983	286	29. Mai	F1S1	0	
MSM78_19-1	24.10.2018 11:06	Gravity corer	on deck	149.5	0	179	58.291.071	106.797	283	29.2	ERROR	0	
MSM78_19-1	24.10.2018 10:58	Gravity corer	hoisting	145.6	0	358	58.291.054	1.068.016	282	25. Mai	F1S1	146	
MSM78_19-1	24.10.2018 10:57	Gravity corer	max depth/on ground	147.6	0	285	58.291.052	1.067.992	281	25. Mai	F1S1	147	
MSM78_19-1	24.10.2018 10:53	Gravity corer	in the water	148.2	0	193	58.291.012	1.068.097	284	28. Feb	F1S1	-8	
MSM78_18-1	24.10.2018 10:11	Gravity corer	on deck	164.9	0	48	58.282.394	0.974616	276	28. Jun	F1S1	-9	
MSM78_18-1	24.10.2018 10:03	Gravity corer	hoisting	166.2	0	267	58.282.419	0.97468	275	24	F1S1	166	
MSM78_18-1	24.10.2018 10:02	Gravity corer	max depth/on ground	163.8	0	38	58.282.403	0.974632	277	24. Jul	F1S1	166	

MSM78_18-1	24.10.2018 09:58	Gravity corer	in the water	164.5	0	290	58.282.408	0.974658	276	26. Jan	F1S1	-6	
MSM78_17-1	24.10.2018 09:40	Gravity corer	on deck	163.6	0	327	58.282.413	0.974638	279	24. Jan	F1S1	-9	
MSM78_17-1	24.10.2018 09:32	Gravity corer	hoisting	166.2	0	164	58.282.408	0.974637	274	22. Aug	F1S1	163	
MSM78_17-1	24.10.2018 09:31	Gravity corer	max depth/on ground	165.4	0	198	58.282.406	0.974605	271	21. Jul	F1S1	163	
MSM78_17-1	24.10.2018 09:26	Gravity corer	in the water	163.2	0	352	58.282.396	0.974601	280	24. Jun	F1S1	-4	
MSM78_16-1	24.10.2018 09:08	Gravity corer	on deck	171.1	0	92	58.281.427	0.970711	278	24. Jul	F1S1	-9	
MSM78_16-1	24.10.2018 09:00	Gravity corer	hoisting	168	0	201	58.281.423	0.970696	277	23. Aug	F1S1	165	
MSM78_16-1	24.10.2018 09:00	Gravity corer	max depth/on ground	169.1	0	254	58.281.438	0.970709	277	24. Jul	F1S1	165	
MSM78_16-1	24.10.2018 08:55	Gravity corer	in the water	169.1	0	184	58.281.421	0.970666	278	24. Jun	F1S1	0	
MSM78_15-1	24.10.2018 08:34	Gravity corer	on deck	170.4	0	172	58.281.445	0.970954	288	19	F1S1	-9	
MSM78_15-1	24.10.2018 08:25	Gravity corer	hoisting	167.8	0	8	58.281.468	0.970913	283	16. Sep	F1S1	165	
MSM78_15-1	24.10.2018 08:24	Gravity corer	max depth/on ground	168	0	303	58.281.461	0.970914	282	18	F1S1	165	
MSM78_15-1	24.10.2018 08:18	Gravity corer	in the water	171.5	0	179	58.281.474	0.970941	275	15. Mrz	F1S1	-5	
MSM78_14-1	24.10.2018 07:29	Gravity corer	on deck	168.2	0	114	58.281.486	0.97094	236	9	F1S1	-8	
MSM78_14-1	24.10.2018 07:20	Gravity corer	hoisting	169.8	0	56	58.281.467	0.970932	239	08. Jun	F1S1	166	
MSM78_14-1	24.10.2018 07:19	Gravity corer	max depth/on ground	170.4	0	184	58.281.483	0.970913	242	07. Sep	F1S1	168	
MSM78_14-1	24.10.2018 07:11	Gravity corer	in the water	168.2	0	169	58.281.468	0.970919	244	07. Aug	F1S1	0	
MSM78_13-1	24.10.2018 06:46	Parasound	profile end	155.6	7	122	58.281.741	0.969614	293	04. Jul	ERROR	0	
MSM78_13-1	24.10.2018 04:45	Parasound	alter course	142.8	6	158	58.399.291	0.577632	332	12. Sep	ERROR	0	rwk=120−
MSM78_13-1	24.10.2018 03:49	Parasound	alter course	141.6	7	114	58.491.063	0.509915	332	14. Feb	ERROR	0	rwk=158−

MSM78_13-1	23.10.2018 08:08	Parasound	information	116.8	7	34	58.254.357	1.331.792	298	33.9	ERROR	0	variable Kurse und Geschv
MSM78_13-1	23.10.2018 07:05	Parasound	alter course	136.4	6	25	58.184.485	1.143.464	289	40.1	ERROR	0	rwk=056−
MSM78_13-1	23.10.2018 06:55	Parasound	alter course	136.7	7	56	58.175.529	1.115.757	292	38.9	ERROR	0	beginn ausweichen Restric
MSM78_13-1	23.10.2018 05:46	Parasound	alter course	141.6	7	82	58.101.098	0.906688	292	39.4	ERROR	0	rwk=056−
MSM78_13-1	23.10.2018 05:30	Parasound	alter course	142.7	7	32	58.093.553	0.849508	282	38	ERROR	0	rwk=079−
MSM78_13-1	23.10.2018 05:05	Parasound	alter course	146.3	7	52	58.058.707	0.792717	285	36.7	ERROR	0	rwk=040−
MSM78_13-1	23.10.2018 04:21	Parasound	alter course	147.3	7	73	58.010.081	0.657872	292	38.2	ERROR	0	rwk=056−
MSM78_13-1	23.10.2018 01:26	Parasound	alter course	120.2	6	247	57.883.189	0.116865	281	38.5	ERROR	0	rwk=068−
MSM78_13-1	22.10.2018 22:32	Parasound	alter course	149.3	5	244	57.990.635	0.608497	268	40.4	ERROR	0	rwk=248−
MSM78_13-1	22.10.2018 21:36	Parasound	alter course	144.5	5	241	58.030.486	0.753408	265	41.3	ERROR	0	rwk=242−
MSM78_13-1	22.10.2018 20:15	Parasound	alter course	177.8	4	258	58.049.798	0.968915	258	39.4	ERROR	0	rwk=261−
MSM78_13-1	22.10.2018 20:03	Parasound	alter course	138.2	7	216	58.074.057	0.981763	263	40.8	ERROR	0	rwk=192−
MSM78_13-1	22.10.2018 15:34	Parasound	information	97.1	6	244	58.269.366	1.601.802	239	42.8	ERROR	0	mit EM 712, rwk 239−
MSM78_12-1	22.10.2018 15:26	Parasound	profile end	96.4	7	119	58.273.887	1.611.315	234	36.9	ERROR	0	
MSM78_12-1	22.10.2018 06:41	Parasound	alter course	122.9	7	94	58.638.833	-0.257553	285	30. Jul	ERROR	0	rwk=110−
MSM78_12-1	22.10.2018 05:19	Parasound	alter course	119.5	6	298	58.641.081	-0.540425	275	31. Mai	ERROR	0	rwk=090−
MSM78_12-1	22.10.2018 03:44	Parasound	alter course	122.6	5	277	58.577.809	-0.275359	275	31. Jul	ERROR	0	rwk=295−
MSM78_12-1	22.10.2018 00:10	Parasound	alter course	139.2	5	293	58.481.323	0.307104	266	41.7	ERROR	0	rwk=288−
MSM78_12-1	21.10.2018 19:23	Parasound	profile start	144.5	5	272	58.292.074	1.076.954	280	31.9	ERROR	0	mit EM712 parallel
MSM78_11-1	21.10.2018 18:46	MEBO Seafloor Drill	information	147.1	0	223	58.291.348	10.667	281	30. Mrz	ERROR	0	Ranger 2 an Deck

MSM78_11-1	21.10.2018 18:45	MEBO Seafloor Drill	information	148.7	0	102	58.291.348	1.066.719	280	30. Mai	ERROR	0	Ger船 zur・k an Deck
MSM78_11-1	21.10.2018 11:36	MEBO Seafloor Drill	End of drilling	148.7	0	302	58.291.373	1.066.734	282	16. Mai	ERROR	0	
MSM78_11-1	20.10.2018 22:12	MEBO Seafloor Drill	Start drilling	148	0	99	58.291.098	1.066.899	236	18. Jul	ERROR	0	
MSM78_11-1	20.10.2018 21:36	MEBO Seafloor Drill	max depth/on ground	148.2	0	330	58.291.098	1.066.898	241	20. Mrz	ERROR	0	
MSM78_11-1	20.10.2018 21:25	MEBO Seafloor Drill	lowering	148.4	0	126	58.291.096	10.669	241	20. Jun	ERROR	0	
MSM78_11-1	20.10.2018 21:22	MEBO Seafloor Drill	information	148.2	0	165	58.291.104	1.066.878	239	20. Jul	ERROR	0	richtiger ger船ename Rock
MSM78_10-1	20.10.2018 18:03	MEBO Seafloor Drill	information	163.4	0	327	58.281.304	0.970243	224	19. Jan	ERROR	0	Ger船 zur・k an Deck
MSM78_10-1	20.10.2018 17:48	MEBO Seafloor Drill	hoisting	163.4	0	51	58.281.313	0.970252	219	18. Apr	ERROR	0	
MSM78_10-1	20.10.2018 15:19	MEBO Seafloor Drill	End of drilling	163.8	0	128	58.281.307	0.97027	208	19. Jan	ERROR	0	
MSM78_10-1	20.10.2018 02:51	MEBO Seafloor Drill	Start drilling	159.6	0	99	58.281.603	0.969811	257	08. Jul	ERROR	0	
MSM78_10-1	20.10.2018 02:17	MEBO Seafloor Drill	max depth/on ground	159.4	0	311	58.281.608	0.969831	254	11. Jan	ERROR	0	
MSM78_10-1	20.10.2018 01:48	MEBO Seafloor Drill	lowering	160.3	0	74	58.281.617	0.969866	263	12. Feb	ERROR	0	
MSM78_10-1	20.10.2018 01:40	MEBO Seafloor Drill	information	159.9	0	299	58.281.616	0.969895	261	13. Jan	ERROR	0	RD2
MSM78_9-1	19.10.2018 23:02	MEBO Seafloor Drill	information	160.1	0	39	58.281.727	0.969863	291	15	ERROR	0	Ger船 zur・k an Deck wg
MSM78_9-1	19.10.2018 22:29	MEBO Seafloor Drill	lowering	160.3	0	6	58.281.728	0.969867	306	14. Jan	ERROR	0	
MSM78_9-1	19.10.2018 22:20	MEBO Seafloor Drill	information	160.7	0	133	5.828.173	0.969866	297	13. Apr	ERROR	0	richtiger Ger船ename Roc
MSM78_8-1	19.10.2018 18:59	MEBO Seafloor Drill	information	160.3	0	114	58.281.682	0.969887	289	18. Jun	ERROR	0	Ger船 zur・k an Deck
MSM78_8-1	19.10.2018 18:46	MEBO Seafloor Drill	hoisting	160.7	0	224	58.281.672	0.969884	291	20. Jul	ERROR	0	
MSM78_8-1	19.10.2018 18:30	MEBO Seafloor Drill	End of drilling	159.2	0	188	58.281.692	0.969916	296	17. Jul	ERROR	0	
MSM78_8-1	19.10.2018 16:14	MEBO Seafloor Drill	Start drilling	160	0	16	58.281.468	0.970017	252	19. Feb	ERROR	0	

MSM78_8-1	19.10.2018 15:55	MEBO Seafloor Drill	max depth/on ground	160.7	0	6	582.815	0.970011	239	20. Mrz	ERROR	0	
MSM78_8-1	19.10.2018 15:40	MEBO Seafloor Drill	information	159.5	0	291	58.281.471	0.970022	242	17. Mrz	ERROR	0	Ger船 RD2 zu Wasser
MSM78_7-1	19.10.2018 13:31	Multibeam Echosounder	profile end	145.2	7	262	58.279.228	0.946098	218	23. Mai	EL2	8626	
MSM78_7-1	19.10.2018 12:50	Multibeam Echosounder	alter course	138	4	262	58.293.058	109.257	212	28. Jan	EL2	109	rwk=259−
MSM78_7-1	19.10.2018 12:19	Multibeam Echosounder	alter course	121.6	6	44	58.301.386	0.987954	216	25. Mrz	EL2	1008	rwk=100−
MSM78_7-1	19.10.2018 11:55	Multibeam Echosounder	alter course	144.9	6	222	58.275.938	0.960584	217	27. Jan	EL2	1529	rwk=042−
MSM78_7-1	19.10.2018 11:37	Multibeam Echosounder	alter course	145.1	5	81	58.295.479	0.984283	201	25. Mai	EL2	1529	rwk=222−
MSM78_7-1	19.10.2018 11:20	Multibeam Echosounder	alter course	146.2	5	325	58.276.076	0.961968	195	29. Mrz	EL2	1529	rwk=042−
MSM78_7-1	19.10.2018 11:05	Multibeam Echosounder	alter course	145.1	5	207	58.289.528	0.988843	199	25. Feb	EL2	1529	rwk=222−
MSM78_7-1	19.10.2018 11:02	Multibeam Echosounder	alter course	144.6	4	89	58.293.006	0.985943	198	29. Jun	EL2	1529	rwk=163−
MSM78_7-1	19.10.2018 10:48	Multibeam Echosounder	alter course	146.2	7	348	58.277.856	0.960014	202	27. Aug	EL2	1529	rwk=042−
MSM78_7-1	19.10.2018 10:44	Multibeam Echosounder	alter course	145.9	5	230	58.273.373	0.966748	198	27. Jun	EL2	1660	rwk=343−
MSM78_7-1	19.10.2018 10:31	Multibeam Echosounder	profile start	145	5	223	58.285.697	0.988242	199	27. Mai	EL2	2136	mit P70, rwk=222−
MSM78_6-1	19.10.2018 10:09	MEBO Seafloor Drill	information	139.6	0	246	58.290.928	1.067.223	199	27. Sep	EL2	2853	Ranger 2 an Deck
MSM78_6-1	19.10.2018 10:07	MEBO Seafloor Drill	information	140.7	0	39	58.290.905	106.721	199	25. Jun	EL2	2925	Ger船 zur・k an Deck
MSM78_6-1	19.10.2018 09:55	MEBO Seafloor Drill	hoisting	139.5	0	169	58.290.932	106.725	208	26. Sep	EL2	3280	
MSM78_6-1	19.10.2018 06:52	MEBO Seafloor Drill	End of drilling	146.9	0	158	58.290.904	1.067.239	210	25. Sep	ERROR	0	
MSM78_6-1	17.10.2018 20:39	MEBO Seafloor Drill	Start drilling	148.4	0	119	58.291.373	1.066.785	279	14	ERROR	0	
MSM78_6-1	17.10.2018 19:38	MEBO Seafloor Drill	max depth/on ground	148	0	271	58.291.362	1.066.783	267	15. Jun	ERROR	0	
MSM78_6-1	17.10.2018 19:28	MEBO Seafloor Drill	lowering	148	0	46	58.291.352	1.066.775	269	16. Sep	ERROR	0	

MSM78_6-1	17.10.2018 19:28	MEBO Seafloor Drill	information	148.4	0	256	58.291.352	1.066.778	269	17. Jan	ERROR	0	Ger船 RD2
MSM78_5-1	17.10.2018 16:39	MEBO Seafloor Drill	information	139.9	0	270	58.291.358	1.066.863	275	16. Apr	ERROR	0	Ger船 zur・k an Deck
MSM78_5-1	17.10.2018 16:39	MEBO Seafloor Drill	hoisting	140.1	0	74	58.291.357	1.066.868	274	16. Mai	ERROR	0	
MSM78_5-1	17.10.2018 16:17	MEBO Seafloor Drill	information	140.5	0	156	58.291.357	1.066.871	269	17. Feb	ERROR	0	tests
MSM78_5-1	17.10.2018 16:06	MEBO Seafloor Drill	lowering	139.6	0	332	58.291.363	106.687	266	15. Jul	ERROR	0	richtiger Ger船ename: RD
MSM78_4-1	17.10.2018 15:07	Parasound	profile end	138.8	5	79	58.292.796	1.082.632	277	16. Jul	ERROR	0	
MSM78_4-1	17.10.2018 14:18	Parasound	profile start	147.1	2	80	58.280.272	0.954982	277	14. Mai	ERROR	0	mit EM712
MSM78_3-1	17.10.2018 13:49	Sound Velocity Profiler	on deck	153.7	0	249	58.284.571	0.98271	279	16. Feb	EL1	-14	
MSM78_3-1	17.10.2018 13:42	Sound Velocity Profiler	max depth/on ground	152.8	0	255	58.284.556	0.982684	285	13. Jun	EL1	150	
MSM78_3-1	17.10.2018 13:36	Sound Velocity Profiler	in the water	153.5	0	198	58.284.555	0.982709	289	14. Jan	EL1	0	
MSM78_2-1	17.10.2018 13:28	Parasound	profile end	146.3	6	52	58.283.346	0.979136	287	16. Feb	EL1	-14	
MSM78_2-1	17.10.2018 11:42	Parasound	alter course	147.1	7	89	58.156.995	0.67561	270	14. Mrz	ERROR	0	rwk=052−
MSM78_2-1	17.10.2018 07:25	Parasound	alter course	121.4	7	65	58.130.522	-0.25958	249	15. Jun	ERROR	0	rwk=087−
MSM78_2-1	17.10.2018 02:54	Parasound	profile start	96.9	0	49	5.762.571	-0.43897	225	22. Apr	ERROR	0	mit EM 712
MSM78_1-1	17.10.2018 02:19	Sound Velocity Profiler	on deck	95	0	244	57.626.029	-0.438478	212	19. Jan	EL1	-14	
MSM78_1-1	17.10.2018 02:13	Sound Velocity Profiler	max depth/on ground	94.9	0	243	57.626.235	-0.438046	211	20. Aug	EL1	95	
MSM78_1-1	17.10.2018 02:08	Sound Velocity Profiler	in the water	95.3	0	82	57.626.239	-0.438202	209	22. Apr	EL1	0	
MSM78_0_Underway-4	25.10.2018 10:35	Multibeam Echosounder	profile end	56.5	11	221	56.451.121	-2.028.672	260	13. Aug	ERROR	0	
MSM78_0_Underway-4	16.10.2018 19:15	Multibeam Echosounder	profile start	58.9	13	39	56.497.134	-2.027.991	206	17. Feb	ERROR	0	
MSM78_0_Underway-3	25.10.2018 12:20	Parasound	profile end	56.3	14	241	56.182.083	-2.458.849	253	23. Jun	ERROR	0	

MSM78_0_Underway-3	16.10.2018 17:24	Parasound	profile start	56.4	13	49	56.181.625	-2.462.562	224	19. Mrz	ERROR	0

Appendix B: Hydroacoustics acquisition protocols

Time UTC	Latitude xx° xx.x‘	Longitude xx° xx.x‘	Course [°]	Heading [°]	Speed O.G. [kn]	Depth EM712 [kn]	Depth SLF [m]	Frequency range EM712	ln cnt	Mode	Line	Waypoint	Remarks
Wednesday, 17.10.2018													
SVP: MSM78_St2_SVP01													
02:55	57° 37.54	0° 26.33	26,90	354,00	0,90	96,50	109,60	40-100		72/72 EQDST Dynamic, Trigger on	1	1	**Start St.2 Hydroacoustic Transect, start logging multibeam (ALL) and parasound**
03:20	57°39.96	0°25.60	9,10	4,20	6,90	103,80	117,10				1		
03:50	57°43.27	0°24.50	9,10	5,30	7,00	102,80	115,80				1		
04:18	57°46.75	0°23.33	10,50	6,40	6,90	103,00	115,90				1		
04:49	57°50.18	0°22.19	10,00	7,10	6,90	101,50	114,40				1		
05:20	57°53.63	0°21.02	8,90	6,60	6,90	109,30	122,10				1		
05:50	57°57.31	0°19.78	8,80	5,70	7,00	112,00	124,80				1		
06:20	58°00.59	0°18.68	9,00	4,20	6,90	117,20	130,50				P001		
06:48	58°03.78	0°17.60	10,20	5,20	7,10	119,80	132,80				1		
07:18	58°07.25	0°16.41	10,30	4,80	7,00	121,00	136,10				1		
07:23	58°07.75	0°15.90	74,50	68,00	6,90	121,30	134,60				P002	2	Start line 2 hydroacoustic transect
07:51	58°07:97	0°09.69	88,00	86,60	7,00	123,50	136,60				2		
08:20	58°08.14	0°03.44	86,00	81,90	7,10	127,80	140,80				2		
08:50	58°08.32	0°06.06	83,30	83,00	7,00	129,70	143,20		0006		2		
09:20	58°08.52	0°09.78	84,70	84,50	7,00	137,40	150,40		0006		2		
09:50	58°08.709	0°16.29	85,20	83,70	7,00	140,30	153,60		0007		2		
10:20	58°08.907	0°22.85	85,70	84,90	7,10	143,10	162,80		0007		2		
10:50	58°09.079	0°28.76	86,10	86,60	6,90	145,60	158,50		0007		2		
11:20	58°09.27	0°35.53	85,50	86,30	7,10	146,00	168,60		0008		2		

11:42	58°09.42	0°40.652	73,00	58,00	6,60	147,70	160,00		0010		P003	3	Start line 3 hydroacoustic transect
12:22	58° 12.29	0° 47.55	51,00	51,00	7,10	149,70	162,30		0010		3		
12:49	58° 14.22	00° 52.15	48,00	50,90	7,00	148,40	161,80		0011		3		
13:21	58°16.52	00° 57.65	50,00	49,00	7,00	147,40	160,50		0011		3		
13:28	58° 17.06	00° 58.88	42,00	42,00	2,70	152,00	159,30					4	end of survey
MSM78_St3_SVP02													
14:18	58° 16.81	0° 57.27	77,20	76,00	1,90	147,10	-		0012	60/60 EQANG Fixed, Trigger off	P004		start logging multibeam EM712 WCI/ALL
14:27	58° 16.94	0° 58.68	82,00	75,00	5,00	145,50			0013	70/70 HD EQDST Dynamic			
15:09	58° 17.55	01° 05.31	151,00	176,00	5,00	146,50			0015				end logging multibeam, start loggin parasound
Friday, 19.10.2018													
10:12	58° 17.40	01° 03.95	218,00	216,00	4,50	139,10	-	40-100	0016	60/60 HDEQDST Single, Trigger off	0	0	start logging multibeam EM712 WCI/ALL, problems with ping rate (0.2-0.3 Hz), most probably a cause of water column imaging and subsequent data storage (range 1880 m), single swath give 0.3 Hz, dual swath 0.15 Hz !!!
10:30	58° 17.23	0° 59.43	221,00	219,00	6,10	146,00			0019		1	1	start survey, start line 1
10:49	58° 16.78	0° 57.688	53,00	49,00	5,90	146,80			0022		2	3	start line 2
11:02	58°17.57	0°59.21	125,00	150,00	3,80	144,60			0022		2	4	end line 2
11:05	58°17.38	0°59.33	207,00	221,00	5,00	144,60			0024		3	5	start line 3
11:19	58° 16.533	0° 57.82	286,00	257,00	4,60	145,60			0025		3	6	eol 3
11:24	58° 16.96	0° 57.68	51,00	44,00	5,80	145,10			0026		4	7	sol4
11:37	58° 17.72	0° 59.09	95,00	126,00	4,80	144,30			0027		4	8	eol4
11:40	58° 17.495	0° 59.23	218,00	225,00	4,70	143,90			0028		5	9	sol5

12:02	58° 16.995	0° 57.393	53,00	51,00	5,30	145,20			0030		6	11	sol6
12:17	58° 16.93	0° 59.03	41,00	36,00	5,20	144,10			0031		6	12	eol12
12:22	58° 18.15	0° 59.81	96,00	105,00	7,20		157,70		-		P005		stop logging multibeam, start logging Parasound
12:47	58° 17.72	1° 05.41	108,00	11,00	6,80		151,90				P005		eol P005
12:50	58° 17.58	1° 05.514	273,00	266,00	4,40		158,00				P006		sol P006
13:09	58° 17.22	0° 01.46	261,00	255,00	7,60		156,40						
13:31	58° 16.75	0° 56.77	261,00	256,00	6,70		160,40				P006		eol P006, sol P007
14:01	58° 17.00	0° 58.42	-	-	-		170,00				P007		eol P007
MSM78_St3_SVP02													
Sunday, 21.10.2018													
19:20	58°17.50	001°05.05	252,00	271,00	3,90	138,80	159,20	40-100	33	70/70 HDEQDST Single Trigger on	8	0	solP008, Parasound file profiles different
19:45	58°17.74	01°00.18	272,00	275,00	6,40	146,50	157,20						
20:15	58°18.03	00°54.44	273,00	277,00	5,70	146,40	160,10				8	1	eolP008
20:17	58°18.15	00°53.98	300,00	289,00	4,70	147,00	159,40		34		9		solP009
20:45	58°19.35	00°49.75	284,00	288,00	5,00	148,00	159,90						
21:00													Trigger every 5 sec
21:06	58°20.27	00°46.82	303,00	302,00	6,20	145,00	160,00						Trigger 'normal' again
21:15	58°20.77	00°45.57	304,00	297,00	4,30	141,10	156,20						
21:44	58°22.19	00°41.05	297,00	294,00	6,00	140,30	154,90						
22:14	58°23.51	00°36.73	299,00	298,00	5,80	142,20	163,80						
22:26	58°24.12	00°34.75	2994,00	292,00	5,40	143,60	163,30		35		10	2	eolP008, solP010
22:51	58° 25.32	00° 30.71	297,00	296,00	6,50	143,90	163,40		36				
23:19	58° 26.67	00° 26.21	298,00	300,00	6,50	144,60	157,50		37				
23:47	58° 27.86	00° 21.97	301,00	291,00	5,30	140,60	152,30		38				
Monday, 22.10.2018													
00:10	58° 28.88	00° 18.409	285,00	283,00	5,10	139,60	152,20		38		11	3	eol P010, solP011
00:39	58° 29.60	00° 14.09	293,00	285,00	3,40	144,00	158,00		39				
01:13	58° 30.56	00° 08.30	288,00	282,00	5,10	140,00	153,00		39				

01:39	58° 31.23	00° 04.198	281,00	282,00	6,90	138,60	152,60		40				
02:07	58° 32.01	00° 00.49	296,00	285,00	5,30	140,10	151,10		40				
02:37	58° 32.821	00° 05.29	282,00	278,00	4,30	135,70	149,70		41				
03:06	58°33.599	00°10.04	296,00	282,00	4,70	132,20	145,60		41				
03:36	58°34.447	00°15.22	290,00	285,00	6,80	128,10	142,30		42				
03:44	58°34.667	00°16.51	280,00	285,00	5,40	123,10	138,10		42			4	
04:06	58°35.585	00°20.39	295,00	292,00	6,80	103,40	119,50		42				
04:36	58°36.710	00°25.153	286,00	291,00	6,50	114,50	127,10		43				
05:06	58°37.944	00°30.32	285,00	285,00	5,30	113,00	127,70		43				
05:19	58°38.474	00°32.48	286,00	290,00	6,60	118,40	132,70		44			5	eol P011
05:25	58°38.845	00°32.84	106,00	111,00	7,80	120,40	134,20		45		12		sol P012
05:55	58°38.411	00°26.23	98,00	91,00	7,00	110,60	124,60		45				
06:25	58°38.349	00°19.33	92,00	88,00	7,40	126,40	140,00		45				
06:41	58°38.330	00°15.38	97,00	94,00	7,20	123,10	138,40		46			6	
07:10	58°37.186	00°09.38	112,00	110,00	7,20	135,50	151,40		46				
07:40	58°35.913	00°02.77	105,20	104,70	6,90	136,80	153,00		47				
08:11	58°36.615	00°03.92	109,00	107,00	7,20	140,80	154,50		47				
08:40	58°33.558	00°10.17	115,00	117,00	7,30	140,90	156,00		48				
09:10	58°32181	00°46.48	110,00	110,00	7,10	142,00	163,00		48				
09:40	58°30.950	00°22.83	109,50	108,00	7,20	139,00	154,00		49				
10:10	58°29.693	00°29.32	114,00	110,00	7,20	139,20	153,60		49				
10:40	58°28.442	00°35.67	110,00	109,00	6,90	143,00	161,00		50			7	
11:10	58° 27.10	00°42.47	109,00	112,00	7,00	141,80	158,00		50				
11:36	58° 26.02	00°48.00	108,00	11,00	7,30	138,90	152,00		51				updated Parasound profile number to 12 (same as line)
12:07	58° 24.76	00°54.382	108,00	109,00	7,60	135,90	147,60		51				
12:34	58° 23.67	01° 00.02	119,00	119,00	7,30	128,00	142,50		52				
13:03	58° 22.43	01° 06.26	111,00	115,00	7,30	136,00	149,90		52				
13:35	58° 21.08	01° 13.08	107,00	114,00	7,60	125,10	141,50		53				
14:02	58° 19.95	01° 18.86	111,00	114,00	7,30	125,40	138,80		53				
14:30	58° 18.81	01° 24.65	109,00	121,00	6,80	113,00	129,00		54				
15:00	58°17.526	01°31.16	109,90	122,60	6,70	104,20	117,70		54				
15:25	58°16.44	01°36.68	119,00	136,00	6,60	100,30	111,50		55			8	eol P012

15:34	58°16.14	01°35.97	256,00	248,00	6,20	99,80	111,40		57		13		sol P013
16:00	58°15.035	01°32.41	232,00	237,00	5,10	99,70	110,80		57				
16:34	58°13.591	01°27.87	243,00	238,00	5,20	97,00	112,80		58				
17:00	58°12.47	01°24.32	238,00	242,00	4,50	106,50	122,60		58				
17:55	58°10.073	01°16.69	249,00	246,00	4,50	123,80	139,70		59				
18:35	58°08.372	01°11.32	239,00	237,00	6,30	134,50	145,10		60				
19:00	58°07.263	01°07.82	237,50	244,00	6,50	136,00	148,90		60				
19:30	58°05.913	1°03.585	242,00	249,00	5,60	136,70	150,30		60				
20:03	58°04.406	00°58.79	216,50	224,00	7,50	137,70	150,70		61		14	9	eol P013, sol P014
20:15	58°02:984	00°58:21	193,00	208,00	7,80	138,00	151,00		61		15	10	eol P014, sol P015
20:30	58°02.782	00°55.767	260,00	265,00	4,20	138,60	151,70		61				
21:00	58°02.389	00°50.89	245,00	258,00	6,60	140,10	155,40		62				
21:34	58°01.938	00°45.523	246,00	264,00	4,70	161,50	159,60		63		16	11	eol P015, sol P016
22:00	58°00.80	00°41.48	251,00	250,00	7,10	145,50	161,90		63				
22:27	57°59.596	00°37.253	250,00	247,00	5,10	147,00	159,00		63		17	12	eol P016, sol P017
23:00	57° 58.44	00° 32.03	242,00	264,00	4,40	144,00	154,00		64				
23:31	57° 57.29	00° 26.68	247,00	259,00	6,10	139,10	150,70		65				
23:54	57° 56.44	00° 22.83	256,00	254,00	5,80	136,00	148,00		65				
Tuesday, 23.10.2018													
00:23	57° 55.37	00° 17.92	251,00	253,00	5,90	133,20	149,80		65				
00:57	57° 54.12	00° 12.17	255,00	260,00	7,00	127,70	138,30		66				
01:25	57° 52.99	00° 07.03	253,00	262,00	6,10	120,20	133,30		67		18	13	eol P017, sol P018
01:37	57° 53.61	00° 06.76	72,00	55,00	7,30	119,00	134,00		68		19	14	eol P018, sol P019
02:04	57° 54.76	00° 12.15	71,00	61,00	7,40	126,10	140,00		68				
02:37	57° 56.10	00° 18.40	65,00	65,00	7,00	136,70	149,90		68				
03:00	57°57.115	00°23.14	62,30	61,60	6,90	135,50	148,60		69				
03:33	57°58.56	00°29.84	60,40	62,30	6,80	140,10	154,30		69				
04:00	57°59.67	00°35.12	61,60	62,80	6,90	145,90	157,60		70				
04:21	58°00.60	00°39.49	78,40	62,10	7,00	147,20	159,80		71		20	15	eol P019, sol P020
04:50	58°02.54	00°44.83	55,00	51,80	7,30	146,10	157,80		71				
05:06	58°03.53	00°47.65	57,50	52,30	7,00	144,80	157,90		72			16	
05:30	58°05.65	00°51.07	49,50	41,90	6,80	144,70	158,60		73			17	
05:46	58°06.07	00°54.51	78,70	71,10	6,60	144,50	156,40		74			18	

06:14	58°07.86	00°59.56	43,30	51,10	7,20	140,50	155,00		74				
06:43	58°09.80	001°04.95	51,00	45,00	7,00	135,90	152,20		74				
06:55	58°10.607	01°07.101	56,00	52,00	6,80	137,00	151,00		76			19	
07:06	58°11.216	01°08.816	50,00	40,00	6,90	135,50	149,90		77			21	
07:34	58°12.980	01°13.735	63,50	53,00	7,20	129,50	143,50		77				
08:00	58°14.615	01°18.265	65,00	49,00	6,70	120,00	133,10		77				
08:09	58°15.34	01°19.95	345,00	335,00	5,90	112,10	126,80		79		21	22	eolP020, solP021
08:30	58°16.226	01°17.90	314,50	299,60	3,00	117,80	127,50		79				
09:02	58°17.425	01°14.315	309,60	302,00	4,40	132,40	143,40		79				
09:30	58°18.64	01°19.04	296,90	304,40	4,60	136,60	146,80		80				
10:00	58°19.85	01°07.66	299,00	300,00	4,60	136,70	147,90		80				
10:30	58°21.17	01°03.94	305,00	302,00	5,70	138,00	156,70		81				
10:55	58°22.26	01°00.68	299,60	301,50	5,40	141,00	153,90		81				
11:25	58° 23.42	00° 56.61	296,00	298,00	5,80	127,60	142,80		82				
12:03	58° 24.76	00° 50.95	304,00	300,00	5,80	137,00	150,00		82				
12:28	58° 25.629	00° 47.55	288,00	298,00	5,30	138,00	152,00		83				
12:55	58° 26.57	00° 43.62	291,00	293,00	5,00	141,00	158,00		83				
13:30	58° 27.64	00° 38.52	296,00	293,00	4,60	146,00	164,00		84				
14:00	58° 28.19	00° 35.73	275,00	288,00	2,90	141,00	157,00		84				
14:33	58° 28.72	00° 32.48	280,00	287,00	3,40	143,00	162,50		85				
14:53	58° 29.16	00° 30.44	297,00	308,00	2,70	140,00	160,00		85				
15:20	58°29.77	00°28.45	270,70	292,40	2,00	138,80	150,50		86				
15:50	58°30.39	00°26.22	304,00	303,00	2,90	136,10	148,90		86				
16:21	58°31.19	00°24.09	307,00	303,00	1,90	137,80	153,70		87				
16:50	58°31.81	00°22.59	301,00	295,00	1,80	139,80	155,30		87				
17:20	58°32.54	00°20.69	294,00	299,00	2,40	139,60	158,70		88				
17:50	58°33.19	00°18.56	299,00	300,00	3,10	139,70	156,40		88				
18:20	58°33.97	00°16.06	302,00	295,00	2,90	142,60	156,50		89				
18:47	58°34.61	00°13.94	303,00	298,00	2,20	142,00	158,00		89				parasound was off duty for 3 min, restarted with trigger box
18:53	58°34.72	00°13.60	304,00	298,00	2,90	142,60	160,10		89				
19:25	58°35.484	00°10.93	296,00	298,30	3,10	141,90	157,00		90				
19:55	58°36.123	00°08.53	299,00	296,10	2,80	141,10	164,10		90				

20:25	58°36.799	00°06.18	287,80	297,40	2,80	141,30	155,90		91				
20:58	58°37.462	00°03.53	283,70	298,90	2,40	140,70	154,20		91				
21:31	58°38.021	00°00.917	305,90	297,60	3,00	141,50	154,30		92				
22:03	58°38.566	00°01.73	287,80	295,80	2,60	140,90	154,00		92				
22:30	58°39.100	00°04.20	300,60	299,10	2,90	138,70	153,70		93				
22:51	58° 39.47	00° 05.78	296,00	298,00	2,80	137,00	151,00		93				large pockmarks
23:39	58° 40.15	00° 08.99	289,00	298,00	2,90	133,00	146,00		94				
23:50	58° 40.52	00° 10.901	300,00	299,00	3,70	132,00	146,00		95		21	23	eolP021
23:57	58° 40.23	00° 11.31	119,00	112,00	6,20	131,00	146,00		96		22		solP022
Wednesday, 24.10.2018													
00:23	58° 39.16	00° 05.84	114,00	109,00	6,50	137,00	151,00		96				
00:53	58° 37.85	00° 00.12	112,00	105,00	5,80	140,00	154,50		96				
01:20	58° 36.78	00° 04.92	117,00	111,00	6,20	143,00	156,00		97				
01:58	58° 35.08	00° 11.19	110,00	114,00	6,10	144,00	157,00		98				
02:27	58° 33.67	00° 15.99	124,00	119,00	5,70	143,00	156,00		98				
02:55	58° 32.17	00° 20.87	118,00	118,00	6,50	141,00	158,00		98				
03:34	58° 30.175	00° 27.86	113,90	116,20	6,60	133,40	148,00		99				
03:53	58° 29.101	00° 30.9	157,50	160,00	6,10	142,30	160,50		99				new direction
04:25	58° 25.871	00° 33.15	158,80	157,70	6,30	143,10	163,60		100				
04:46	58° 23.882	00° 34.80	122,70	116,50	5,80	144,10	161,70		100				new direction
05:19	58° 21.937	00° 41.65	121,30	119,20	7,80	138,50	152,90		101				
05:51	58° 20.037	00° 47.91	116,60	119,80	6,50	142,70	157,30		101				
06:23	58° 18.236	00° 53.85	114,70	122,10	6,90	145,30	158,30		102				
06:55	58°16.88	00°58.27	359,00	272,00	0,90	161,60	176,50		102		22		eolP022, stopped parasound and multibeam
MSM78_St21_SVP03													
12:56	58° 16.89	00° 58.27	137,00	293,00	0,90	-	176,50		--	switched off			start logging parasound, sol P023
13:23	58° 19.032	00° 58.27	8,00	344,00	4,90		157,80						
13:50	58° 21.54	00° 58.25	354,00	346,00	6,90		156,50						
14:25	58° 24.71	00° 58.25	12,00	354,00	7,10		140,00						eolP023, solP024
14:51	58° 23.10	00° 58.35	199,00	204,00	6,70		143,60						
15:29	58° 18.77	00° 55.98	213,00	216,00	6,70		158,20						

15:59	58°16.04	00°52.66	214,70	229,30	5,40		161,00						
15:29	58°14.88	00°49.09	215,70	230,40	5,30		160,50						
15:59	58°13.06	00°45.33	215,00	227,00	5,30		160,60						

Appendix C: Pore water and sediment sampling (DIC = dissolved inorganic carbon, TA= Total alkalinity, Isotopes = δ^{13}-C_{DIC}; Methane 1 = Methane concentration, Methane 2 = Methane isotopic composition, NA = not available)

MSM78-06: Reference Site

Section depth	depth porewater (cm)	Interval	Cations	Anions/H2S	DIC	TA	Isotopes	Nutrients	depth sediment (cm)	Methane 1	Methane 2	Micorbio RNA	Micorbio D_N_A	porosity pot no	Redox sensitive	PFC
MSM78-06-1	111	30	1	901	1	1	1	1	114	1	1			710	1	1
MSM78-06-2	141	60	2	902	2	2	2	2	144	2				711	2	
MSM78-06-2	202	30	3	903	3	3	3	3	205	3	3			701	3	3
MSM78-06-2	232	60	4	904	4	4	4	4	235	4				720	4	
MSM78-06-2	262	90	5	905	5	5	5	5	265	5				721	5	
MSM78-06-2	292	120	6	906	6	6	6	6	295	6				707	6	
MSM78-06-2	322	150	7	907	7	7	7	7	325	7				709	7	
MSM78-06-3	399	30	NA	NA	NA	NA	NA	NA	402	8	8			712	8	8
MSM78-06-3	429	60	9	909	9	9		9	432	9				719	9	
MSM78-06-3	459	90	10	910	10	10		10	462	10		10	10	722	10	
MSM78-06-3	489	120	11	911	11	11		11	492	11				703	11	
MSM78-06-3	550	30	12	912	12	12	12	12	553	12	12			708	12	12
MSM78-06-4	580	60	13	913	13	not full		13	583	13				713	13	
MSM78-06-4	610	90	14	914	NA	not full		14	613	14				718	14	

MSM78-06-4	640	120	15	915	NA	NA		15	643	15				723	15	
MSM78-06-4	670	150	16	916	16	16			673	16				724	16	
MSM78-06-5	717	30	17	917	17	not full		17	720	17	17			717	17	17
MSM78-06-5	747	60	18	918	18	not full		18	750	18				714	18	
MSM78-06-5	777	90	19	919	19	19		19	780	19				707	19	
MSM78-06-5	807	120	20	920	20	20		20	810	20		20	20	704	20	
MSM78-06-5	837	150	21	921	21	21		21	840	21				725	21	
MSM78-06-6	1014	30	22	922	22	22		22	1017	22	22			716	22	22
MSM78-06-7	1124	30	23	923	23	not full		23	1127	23	23			715	23	23
MSM78-06-7	1154	60	24	924	24	not full			1157	24				706	24	
MSM78-06-7	1184	90	25	925	25	not full			1187	25				705	25	
MSM78-06-8	1345	30	26	926	26			26	1348	26	26			661	26	26
MSM78-06-9	1465	30	27	927	27	not full			1468	27	27			too soupy	27	27
MSM78-06-9	1495	60	28	932	NA	NA			1498	28				662	28	
MSM78-06-9	1525	90	29	933	NA	NA		29	1528	29				663	29	
MSM78-06-10	1695	20	30	934	NA	NA		30	1698	30	30	30	30	670	30	30
MSM78-06-11	1874	20	31	931	31	31	31	31	1877	31	31			665	31	31
MSM78-06-12	2030	30	32	925	NA	NA		32	2033	32	32			664	32	32
MSM78-06-13	2154	30	33	936	NA	NA			2157	33	33			666	33	33
MSM78-06-13	2184	60	34	937	NA	NA			2187	34				675	34	
MSM78-06-13	2204	80	35	empty	NA	NA	NA	NA	2207	35				667	35	
MSM78-06-14	2335	30	36	938	NA	NA			2338	36	36			668	36	36

MSM78-06-14	2365	60	37	939	NA	NA			2368	37				669	37	

MSM78-08: Scanner Pockmark

Section depth	depth porewater (cm)	Interval	Cations	Anions/H2S	DIC	TA	Isotopes	Nutrients	depth sediment (cm)	Methane 1	Methane 2	Micorbio RNA	Micorbio D_N_A	porosity pot no	Redox sensitive	PFC
MSM78-08-1	101	30	1	908	1	1	1	1	104	1	1			767	1	
MSM78-08-1	264	30	2	928	2			2	267	2				765	2	
MSM78-08-2	294	60	3	929	3			3	297	3				779	3	
MSM78-08-2	324	90	4	930	4			4	327	4	4			775	4	

MSM78-10: Pockmark

Section depth	depth porewater (cm)	Interval	Cations	Anions/H2S	DIC	TA	Isotopes	Nutrients	depth sediment (cm)	Methane 1	Methane 2	Micorbio RNA	Micorbio D_N_A	porosity pot no	Redox sensitive	PFC	pH
1	130	130	1	940	1	1	1		133	1		1	1	744	1	1	7.24
1	155	25	2	941	2	2			158	2	2			750	2		7.70
2	218	63	3	NA				3	221	3		3	3	771	3		7.70
2	248	30	4	942	4	4		4	251	4	4			743	4		7.80
2	278	30	5	943				5	281	5				753	5	5.00	7.90
2	303	25	6	944	6			6	306	6	6			741	6		7.60
2	328	25	7	951				7	331	7				742	7		7.90

4	555	227	8	945				8	558	8	8			748	8		7.60
4	585	30	9	946				9	588	9		9	9	764	9		7.40
4	615	30	NA	952	10			10	618	10	10			749	10	10	7.40
4	645	30	11	947				11	648	11				745	11		7.50
4	670	25	12	948	12			12	673	12	12			747	12		
6	932	262	NA	NA				13	935	13				754	13		7.20
6	957	25	14	949				14	960	14	14			769	14		7.40
6	987	30	a drop						990	15		15	15	752	15	15.00	7.40
6	1017	30	NA	950				16	1020	16	16			756	16		7.40

MSM78-11: Reference site

Section depth	**depth porewater (cm)**	**Interval**	Cations	Anions/H2S	DIC	TA	Isotopes	Nutrients	**depth sediment (cm)**	Methane 1	Methane 2	Micorbio RNA	Micorbio D_N_A	porosity pot no	Redox sensitive	PFC	pH
MSM78-11-19	130	130	1	953		1			3331	1	1			will be done at home	1		
MSM78-11-20	155	25							3400	2	2				2		
MSM78-11-20	218	63							3420	3					3		

MSM78-14: Pockmark

Section	depth porewater (cm)	Cations	Anions/H2S	DIC	TA	Isotopes	Nutrients	depth sediment (cm)	Methane 1	Methane 2	Micorbio RNA	Micorbio D_N_A	porosity pot no	Redox sensitive
4	10	1	960	1	1	1	1	13	1				700	1
4	20	2	961	2	2	2	2	23	2				691	2
4	30	3	962	3	3	3	3	33	3				690	3
4	40	4	963	4	4	4	4	43	4	4	4		681	4
4	50	5	964	5	5	5	5	53	5				680	5
3	68	6	994	6	6	6	6	71	6				699	6
3	78	7	995	7	7	7	7	81	7				692	7
3	88	8	965	8	8	8	8	91	8	8	8		689	8
3	98	9	996	9	9	9	9	101	9				682	9
3	108	10	997	10	10	NA	10	111	10				679	10
3	138	11	998	NA	11	NA	11	141	11				678	11
2	168	12	808	12	12	NA	12	171	12	12	12		683	12
2	198	13	822	13	13	13	13	201	13				688	13
2	228	14	823	14	14	NA	14	231	14				693	14
1	268	15	824	15	15	NA	15	271	15				698	15

1	301	16	825	16	NA	NA	16	304	16	16	16		138	16
1	328	17	826	17	NA	NA	17	331	17				697	17
4	10	1	960	1	1	1	1	13	1				700	1

MSM78-16: Pockmark

Section	**depth porewater (cm)**	Cations	Anions/H2S	DIC	TA	Isotopes	Nutrients	**depth sediment (cm)**	Methane 1	Methane 2	Micorbio RNA	Micorbio D_N_A	porosity pot no	Redox sensitive
4	10	1	954	1	1	1	1	13	1				694	1
3	28	2	955	2	2	2	2	31	2				687	2
3	38	3	956	3	3	3	3	41	3				727	3
3	48	4	957	4	4	4	4	51	4				730	4
3	58	5	958	5	5	5	5	61	5	5	5	5	736	5
3	68	6	959	6	6	6	6	71	6				737	6
3	78	7	809	7			7	81	7				738	7
3	88	8	810	8			8	91	8				731	8
3	98	9	811, 875	9			9	101						
3	108	10	814	10			10	111						
2	148	11	816	11				151	11	11	11	11	733	11
2	178	12	817	12			12	181	12				729	12
2	208	13	818	13				211	13				740	13
1	258	14	819	14	14		14	261	14				735	14

1	288	15	820	15			15	291	15	15	15	15	728	15
1	318	16	821	16				321	16				739	16

MSM78-18: Pockmark

Section	**depth porewater (cm)**	Cations	Anions/H2S	DIC	TA	Isotopes	Nutrients	**depth sediment (cm)**	Methane 1	Methane 2	Micorbio RNA	Micorbio D_N_A	porosity pot no	Redox sensitive
5	10	1	966	1	1	1	1	13	1				778	1
5	20	2	967	2	2	2	2	23	2				671	2
5	30	3	968	3	3	3	3	33	3				755	3
5	40	4	969	4	4	4	4	43	4	4			766	4
5	50	5	970	5	5	5	5	53	5				673	5
5	60	6	971	6	6	6	6	63	6				672	6
5	70	7	972	7	7	7	7	73	7				773	7
4	112	8	974	8	8	8	8	115	8	8			763	8
4	142	9	973	9	9	9	9	145	9				761	9
4	172	10	975	10	10		10	175	10				774	10
3	212	11	976	11	11	11	11	215	11				776	11
3	242	12	999	12	12	12	12	245	12	12			759	12
3	272	13	1000	13	13	13	13	275	13				762	13
2	312	14	801	14	14		14	315	14				760	14

2	342	15	802	15	15	15	15	345	15				772	15
2	372	16	803	16	16	16	16	375	16	16			751	16
1	417	17	812	17	17		17	420	17				770	17
1	442	18	813		18		18	445	18				768	18
1	472	NO SEDIMENT												

MSM78-20: Reference site

Section	**depth porewater (cm)**	Cations	Anions/H2S	DIC	TA	Isotopes	Nutrients	**depth sediment (cm)**	Methane 1	Methane 2	Micorbio RNA	Micorbio D_N_A	porosity pot no	Redox sensitive
6	5	1	977	1	1	1	1	8	1				726	1
5	25	2	978	2	2	2	2	28	2				777	2
5	35	3	979	3	3	3	3	38	3				732	3
5	45	4	980	4	4	4	4	48	4	4	4		455	4
5	55	5	981	5	5		5	58	5				780	5
5	65	6	982	6	6	6	6	68	6				655	6
5	75	7	983	7	7	7	7	78	7				620	7
5	85	8	984	8	8	8	8	88	8	8	8		136	8
5	95	9	985	9	9	9	9	98	9				126	9
5	105	10	986	10	10	10	10	108	10				130	10
4	145	11	987	11	11	11	11	148	11				757	11

4	175	12	988	12	12	12	12	178	12	12	12		674	12
4	205	13	989	13	13	13	13	208	13				69	13
3	245	14	990	14	14	14	14	248	14				651	14
3	275	15	991	15	15	15	15	278	15				134	15
3	305	16	992	16	16	16	16	308	16	16	16		502	16
2	345	17	804	17	17	17	17	348	17				527	17
2	375	18	805	18	18	18	18	378	18				145	18
2	405	19	993	19	19	19	19	408	19				616	19
1	450	20	806	20	20	20	20	453	20	20	20		128	20
1	475	21	807	21	21	21		478	21				653	21
1	505	22				22		508	22				658	22

GEOMAR
Helmholtz-Zentrum für Ozeanforschung Kiel

GEOMAR Reports

No.	Title
1	FS POSEIDON Fahrtbericht / Cruise Report POS421, 08. – 18.11.2011, Kiel - Las Palmas, Ed.: T.J. Müller, 26 pp, DOI: 10.3289/GEOMAR_REP_NS_1_2012
2	Nitrous Oxide Time Series Measurements off Peru – A Collaboration between SFB 754 and IMARPE –, Annual Report 2011, Eds.: Baustian, T., M. Graco, H.W. Bange, G. Flores, J. Ledesma, M. Sarmiento, V. Leon, C. Robles, O. Moron, 20 pp, DOI: 10.3289/GEOMAR_REP_NS_2_2012
3	FS POSEIDON Fahrtbericht / Cruise Report POS427 – Fluid emissions from mud volcanoes, cold seeps and fluid circulation at the Don-_Kuban deep sea fan (Kerch peninsula, Crimea, Black Sea) – 23.02. – 19.03.2012, Burgas, Bulgaria - Heraklion, Greece, Ed.: J. Bialas, 32 pp, DOI: 10.3289/GEOMAR_REP_NS_3_2012
4	RV CELTIC EXPLORER EUROFLEETS Cruise Report, CE12010 – ECO2@NorthSea, 20.07. – 06.08.2012, Bremerhaven – Hamburg, Eds.: P. Linke et al., 65 pp, DOI: 10.3289/GEOMAR_REP_NS_4_2012
5	RV PELAGIA Fahrtbericht / Cruise Report 64PE350/64PE351 – JEDDAH-TRANSECT -, 08.03. – 05.04.2012, Jeddah – Jeddah, 06.04 - 22.04.2012, Jeddah – Duba, Eds.: M. Schmidt, R. Al-Farawati, A. Al-Aidaroos, B. Kürten and the shipboard scientific party, 154 pp, DOI: 10.3289/GEOMAR_REP_NS_5_2013
6	RV SONNE Fahrtbericht / Cruise Report SO225 - MANIHIKI II Leg 2 The Manihiki Plateau - Origin, Structure and Effects of Oceanic Plateaus and Pleistocene Dynamic of the West Pacific Warm Water Pool, 19.11.2012 - 06.01.2013 Suva / Fiji – Auckland / New Zealand, Eds.: R. Werner, D. Nürnberg, and F. Hauff and the shipboard scientific party, 176 pp, DOI: 10.3289/GEOMAR_REP_NS_6_2013
7	RV SONNE Fahrtbericht / Cruise Report SO226 – CHRIMP CHatham RIse Methane Pockmarks, 07.01. - 06.02.2013 / Auckland – Lyttleton & 07.02. – 01.03.2013 / Lyttleton – Wellington, Eds.: Jörg Bialas / Ingo Klaucke / Jasmin Mögeltönder, 126 pp, DOI: 10.3289/GEOMAR_REP_NS_7_2013
8	The SUGAR Toolbox - A library of numerical algorithms and data for modelling of gas hydrate systems and marine environments, Eds.: Elke Kossel, Nikolaus Bigalke, Elena Piñero, Matthias Haeckel, 168 pp, DOI: 10.3289/GEOMAR_REP_NS_8_2013
9	RV ALKOR Fahrtbericht / Cruise Report AL412, 22.03.-08.04.2013, Kiel – Kiel. Eds: Peter Linke and the shipboard scientific party, 38 pp, DOI: 10.3289/GEOMAR_REP_NS_9_2013
10	Literaturrecherche, Aus- und Bewertung der Datenbasis zur Meerforelle (Salmo trutta trutta L.) Grundlage für ein Projekt zur Optimierung des Meerforellenmanagements in Schleswig-Holstein. Eds.: Christoph Petereit, Thorsten Reusch, Jan Dierking, Albrecht Hahn, 158 pp, DOI: 10.3289/GEOMAR_REP_NS_10_2013
11	RV SONNE Fahrtbericht / Cruise Report SO227 TAIFLUX, 02.04. – 02.05.2013, Kaohsiung – Kaohsiung (Taiwan), Christian Berndt, 105 pp, DOI: 10.3289/GEOMAR_REP_NS_11_2013
12	RV SONNE Fahrtbericht / Cruise Report SO218 SHIVA (Stratospheric Ozone: Halogens in a Varying Atmosphere), 15.-29.11.2011, Singapore - Manila, Philippines, Part 1: SO218- SHIVA Summary Report (in German), Part 2: SO218- SHIVA English reports of participating groups, Eds.: Birgit Quack & Kirstin Krüger, 119 pp, DOI: 10.3289/GEOMAR_REP_NS_12_2013
13	KIEL276 Time Series Data from Moored Current Meters. Madeira Abyssal Plain, 33°N, 22°W, 5285 m water depth, March 1980 – April 2011. Background Information and Data Compilation. Eds.: Thomas J. Müller and Joanna J. Waniek, 239 pp, DOI: 10.3289/GEOMAR_REP_NS_13_2013

GEOMAR
Helmholtz-Zentrum für Ozeanforschung Kiel

GEOMAR Reports

No.	Title
14	RV POSEIDON Fahrtbericht / Cruise Report POS457: ICELAND HAZARDS Volcanic Risks from Iceland and Climate Change:The Late Quaternary to Anthropogene Development Reykjavík / Iceland – Galway / Ireland, 7.-22. August 2013. Eds.: Reinhard Werner, Dirk Nürnberg and the shipboard scientific party, 88 pp, DOI: 10.3289/GEOMAR_REP_NS_14_2014
15	RV MARIA S. MERIAN Fahrtbericht / Cruise Report MSM-34 / 1 & 2, SUGAR Site, Varna – Varna, 06.12.13 – 16.01.14. Eds: Jörg Bialas, Ingo Klaucke, Matthias Haeckel, 111 pp, DOI: 10.3289/GEOMAR_REP_NS_15_2014
16	RV POSEIDON Fahrtbericht / Cruise Report POS 442, "AUVinTYS" High-resolution geological investigations of hydrothermal sites in the Tyrrhenian Sea using the AUV "Abyss", 31.10. – 09.11.12, Messina – Messina, Ed.: Sven Petersen, 32 pp, DOI: 10.3289/GEOMAR_REP_NS_16_2014
17	RV SONNE, Fahrtbericht / Cruise Report, SO 234/1, "SPACES": Science or the Assessment of Complex Earth System Processes, 22.06. – 06.07.2014, Walvis Bay / Namibia - Durban / South Africa, Eds.: Reinhard Werner and Hans-Joachim Wagner and the shipbord scientific party, 44 pp, DOI: 10.3289/GEOMAR_REP_NS_17_2014
18	RV POSEIDON Fahrtbericht / Cruise Report POS 453 & 458, "COMM3D", Crustal Structure and Ocean Mixing observed with 3D Seismic Measurements, 20.05. – 12.06.2013 (POS453), Galway, Ireland – Vigo, Portugal, 24.09. – 17.10.2013 (POS458), Vigo, Portugal – Vigo, Portugal, Eds.: Cord Papenberg and Dirk Klaeschen, 66 pp, DOI: 10.3289/GEOMAR_REP_NS_18_2014
19	RV POSEIDON, Fahrtbericht / Cruise Report, POS469, "PANAREA", 02. – 22.05.2014, (Bari, Italy – Malaga, Spain) & Panarea shallow-water diving campaign, 10. – 19.05.2014, Ed.: Peter Linke, 55 pp, DOI: 10.3289/GEOMAR_REP_NS_19_2014
20	RV SONNE Fahrtbericht / Cruise Report SO234-2, 08.-20.07.2014, Durban, -South Africa - Port Louis, Mauritius, Eds.: Kirstin Krüger, Birgit Quack and Christa Marandino, 95 pp, DOI: 10.3289/GEOMAR_REP_NS_20_2014
21	RV SONNE Fahrtbericht / Cruise Report SO235, 23.07.-07.08.2014, Port Louis, Mauritius to Malé, Maldives, Eds.: Kirstin Krüger, Birgit Quack and Christa Marandino, 76 pp, DOI: 10.3289/GEOMAR_REP_NS_21_2014
22	RV SONNE Fahrtbericht / Cruise Report SO233 WALVIS II, 14.05-21.06.2014, Cape Town, South Africa - Walvis Bay, Namibia, Eds.: Kaj Hoernle, Reinhard Werner, and Carsten Lüter, 153 pp, DOI: 10.3289/GEOMAR_REP_NS_22_2014
23	RV SONNE Fahrtbericht / Cruise Report SO237 Vema-TRANSIT Bathymetry of the Vema-Fracture Zone and Puerto Rico TRench and Abyssal AtlaNtic BiodiverSITy Study, Las Palmas (Spain) - Santo Domingo (Dom. Rep.) 14.12.14 - 26.01.15, Ed.: Colin W. Devey, 130 pp, DOI: 10.3289/GEOMAR_REP_NS_23_2015
24	RV POSEIDON Fahrtbericht / Cruise Report POS430, POS440, POS460 & POS467 Seismic Hazards to the Southwest of Portugal; POS430 - La-Seyne-sur-Mer - Portimao (7.4. - 14.4.2012), POS440 - Lisbon - Faro (12.10. - 19.10.2012), POS460 - Funchal - Portimao (5.10. - 14.10.2013), POS467 - Funchal - Portimao (21.3. - 27.3.2014), Ed.: Ingo Grevemeyer, 43 pp, DOI: 10.3289/GEOMAR_REP_NS_24_2015
25	RV SONNE Fahrtbericht / Cruise Report SO239, EcoResponse Assessing the Ecology, Connectivity and Resilience of Polymetallic Nodule Field Systems, Balboa (Panama) – Manzanillo (Mexico), 11.03. -30.04.2015, Eds.: Pedro Martínez Arbizu and Matthias Haeckel, 204 pp, DOI: 10.3289/GEOMAR_REP_NS_25_2015

GEOMAR
Helmholtz-Zentrum für Ozeanforschung Kiel

GEOMAR Reports

No.	Title
26	RV SONNE Fahrtbericht / Cruise Report SO242-1, JPI OCEANS Ecological Aspects of Deep-Sea Mining, DISCOL Revisited, Guayaquil - Guayaquil (Equador), 29.07.-25.08.2015, Ed.: Jens Greinert, 290 pp, DOI: 10.3289/GEOMAR_REP_NS_26_2015
27	RV SONNE Fahrtbericht / Cruise Report SO242-2, JPI OCEANS Ecological Aspects of Deep-Sea Mining DISCOL Revisited, Guayaquil - Guayaquil (Equador), 28.08.-01.10.2015, Ed.: Antje Boetius, 552 pp, DOI: 10.3289/GEOMAR_REP_NS_27_2015
28	RV POSEIDON Fahrtbericht / Cruise Report POS493, AUV DEDAVE Test Cruise, Las Palmas - Las Palmas (Spain), 26.01.-01.02.2016, Ed.: Klas Lackschewitz, 17 pp, DOI: 10.3289/GEOMAR_REP_NS_28_2016
29	Integrated German Indian Ocean Study (IGIOS) - From the seafloor to the atmosphere - A possible German contribution to the International Indian Ocean Expedition 2 (IIOE-2) programme – A Science Prospectus, Eds.: Bange, H.W. , E.P. Achterberg, W. Bach, C. Beier, C. Berndt, A. Biastoch, G. Bohrmann, R. Czeschel, M. Dengler, B. Gaye, K. Haase, H. Herrmann, J. Lelieveld, M. Mohtadi, T. Rixen, R. Schneider, U. Schwarz-Schampera, J. Segschneider, M. Visbeck, M. Voß, and J. Williams, 77pp, DOI: 10.3289/GEOMAR_REP_NS_29_2016
30	RV SONNE Fahrtbericht / Cruise Report SO249, BERING – Origin and Evolution of the Bering Sea: An Integrated Geochronological, Volcanological, Petrological and Geochemical Approach, Leg 1: Dutch Harbor (U.S.A.) - Petropavlovsk-Kamchatsky (Russia), 05.06.2016-15.07.2016, Leg 2: Petropavlovsk-Kamchatsky (Russia) - Tomakomai (Japan), 16.07.2016-14.08.2016, Eds.: Reinhard Werner, et al., DOI: 10.3289/GEOMAR_REP_NS_30_2016
31	RV POSEIDON Fahrtbericht/ Cruise Report POS494/2, HIERROSEIS Leg 2: Assessment of the Ongoing Magmatic-Hydrothermal Discharge of the El Hierro Submarine Volcano, Canary Islands by the Submersible JAGO, Valverde – Las Palmas (Spain), 07.02.-15.02.2016, Eds.: Hannington, M.D. and Shipboard Scientific Party, DOI: 10.3289/GEOMAR_REP_NS_31_2016
32	RV METEOR Fahrtbericht/ Cruise Report M127, Extended Version, Metal fluxes and Resource Potential at the Slow-spreading TAG Midocean Ridge Segment (26°N, MAR) – Blue Mining@Sea, Bridgetown (Barbados) – Ponta Delgada (Portugal) 25.05.-28.06.2016, Eds.: Petersen, S. and Shipboard Scientific Party, DOI: 10.3289/GEOMAR_REP_NS_32_2016
33	RV SONNE Fahrtbericht/Cruise Report SO244/1, GeoSEA: Geodetic Earthquake Observatory on the Seafloor, Antofagasta (Chile) – Antofagasta (Chile), 31.10.-24.11.2015, Eds.: Jan Behrmann, Ingo Klaucke, Michal Stipp, Jacob Geersen and Scientific Crew SO244/1, DOI: 10.3289/GEOMAR_REP_NS_33_2016
34	RV SONNE Fahrtbericht/Cruise Report SO244/2, GeoSEA: Geodetic Earthquake Observatory on the Seafloor, Antofagasta (Chile) – Antofagasta (Chile), 27.11.-13.12.2015, Eds.: Heidrun Kopp, Dietrich Lange, Katrin Hannemann, Anne Krabbenhoeft, Florian Petersen, Anina Timmermann and Scientific Crew SO244/2, DOI: 10.3289/GEOMAR_REP_NS_34_2016
35	RV SONNE Fahrtbericht/Cruise Report SO255, VITIAZ – The Life Cycle of the Vitiaz-Kermadec Arc / Backarc System: from Arc Initiation to Splitting and Backarc Basin Formation, Auckland (New Zealand) - Auckland (New Zealand), 02.03.-14.04.2017, Eds.: Kaj Hoernle, Folkmar Hauff, and Reinhard Werner with contributions from cruise participants, DOI: 10.3289/GEOMAR_REP_NS_35_2017

GEOMAR
Helmholtz-Zentrum für Ozeanforschung Kiel

GEOMAR Reports

No.	Title
36	RV POSEIDON Fahrtbericht/Cruise Report POS515, CALVADOS - CALabrian arc mud VolcAnoes: Deep Origin and internal Structure, Dubrovnik (Croatia) – Catania (Italy), 18.06.-13.07.2017, Eds.: M. Riedel, J. Bialas, A. Krabbenhoeft, V. Bähre, F. Beeck, O. Candoni, M. Kühn, S. Muff, J. Rindfleisch, N. Stange, DOI: 10.3289/GEOMAR_REP_NS_36_2017
37	RV MARIA S. MERIAN Fahrtbericht/Cruise Report MSM63, PERMO, Southampton – Southampton (U.K.), 29.04.-25.05.2017, Eds.: Christian Berndt and Judith Elger with contributions from cruise participants C. Böttner, R.Gehrmann, J. Karstens, S. Muff, B. Pitcairn, B. Schramm, A. Lichtschlag, A.-M. Völsch, DOI: 10.3289/GEOMAR_REP_NS_37_2017
38	RV SONNE Fahrtbericht/Cruise Report SO258/1, INGON: The Indian - Antarctic Break-up Engima, Fremantle (Australia) - Colombo (Sri Lanka), 07.06.-09.07.2017, 29.04.-25.05.2017, Eds.: Reinhard Werner, Hans-Joachim Wagner, and Folkmar Hauff with contributions from cruise participants, DOI: 10.3289/GEOMAR_REP_NS_38_2017
39	RV POSEIDON Fahrtbericht/Cruise Report POS509, ElectroPal 2: Geophysical investigations of sediment hosted massive sulfide deposits on the Palinuro Volcanic Complex in the Tyrrhenian Sea, Malaga (Spain) – Catania (Italy), 15.02.-03.03.2017, Ed.: Sebastian Hölz, DOI: 10.3289/GEOMAR_REP_NS_39_2017
40	RV POSEIDON Fahrtbericht/Cruise Report POS518, Baseline Study for the Environmental Monitoring of Subseafloor CO_2 Storage Operations, Leg 1: Bremerhaven – Bremerhaven (Germany), 25.09.-11.10.2017, Leg 2: Bremerhaven – Kiel (Germany), 12.10.-28.10.2017, Eds.: Peter Linke and Matthias Haeckel, DOI: 10.3289/GEOMAR_REP_NS_40_2018
41	RV MARIA S. MERIAN Fahrtbericht/Cruise Report MSM71, LOBSTER: Ligurian Ocean Bottom Seismology and Tectonics Research, Las Palmas (Spain) – Heraklion (Greece), 07.02.-27.02.2018, Eds.: H. Kopp, D. Lange, M. Thorwart, A. Paul, A. Dannowski, F. Petersen, C. Aubert, F. Beek, A. Beniest, S. Besançon, A. Brotzer, G. Caielli, W. Crawford, M. Deen, C. Lehmann, K. Marquardt, M. Neckel, L. Papanagnou, B. Schramm, P. Schröder, K.-P. Steffen, F. Wolf, Y. Xia, DOI: 10.3289/GEOMAR_REP_NS_41_2018
42	RV METEOR Fahrtbericht/Cruise Report M143, SLOGARO: Slope failures and active gas expulsion along the Romanian margin – investigating relations to gas hydrate distribution, Varna (Romania) – Heraklion (Greece), 12.12.-22.12.2017, Eds.: M. Riedel, F. Gausepohl, I. Gazis, L. Hähnel, M. Kampmeier, P. Urban, J. Bialas, DOI: 10.3289/GEOMAR_REP_NS_42_2018
43	RV POSEIDON Fahrtbericht/Cruise Report POS510, ANYDROS: Rifting and Hydrothermal Activity in the Cyclades Back-arc Basin, Catania (Italy) – Heraklion (Greece), 06.03.-29.03.2017, Ed.: M.D. Hannington, DOI: 10.3289/GEOMAR_REP_NS_43_2018
44	RV POSEIDON Fahrtbericht/Cruise Report POS524, GrimseyEM: Geophysical and geological investigations in the vicinity of the Grimsey Hydrothermal Field offshore Northern Iceland for the assessment of the geothermal potential and the exploration for potential mineralizations within the seafloor, Reykjavik (Iceland) – Bergen (Norway), 7.6 - 26.6.2018, Eds.: Sebastian Hölz and Sofia Martins, DOI: 10.3289/GEOMAR_REP_NS_44_2018
45	RV POSEIDON Fahrtbericht/Cruise Report POS527, Baseline Study for the Environmental Monitoring of Subseafloor CO_2 Storage Operations, Kiel – Kiel (Germany), 15.8. - 3.9.2018, Eds.: Eric Achterberg and Mario Esposito, DOI: 10.3289/GEOMAR_REP_NS_45_2018

GEOMAR
Helmholtz-Zentrum für Ozeanforschung Kiel

GEOMAR Reports

No.	Title
46	RV SONNE Fahrtbericht/Cruise Report SO264, SONNE-EMPEROR: The Plio/Pleistocene to Holocene development of the pelagic North Pacific from surface to depth – assessing its role for the global carbon budget and Earth´s climate, Suva (Fiji) – Yokohama (Japan), 30.6. – 24.8.2018 Ed.: Dirk Nürnberg, DOI: 10.3289/GEOMAR_REP_NS_46_2018
47	RV SONNE Fahrtbericht/Cruise Report SO265, SHATSKY EVOLUTION: Evolution of the Shatsky Rise Hotspot System, Yokohama (Japan) – Kaohsiung (Taiwan), 26.08. – 11.10.2018, Eds.: Jörg Geldmacher, Reinhard Werner, and Folkmar Hauff with contributions from cruise participants, DOI: 10.3289/GEOMAR_REP_NS_47_2018
48	RV MARIA S. MERIAN Fahrtbericht/Cruise Report MSM78, PERMO 2, Edinburgh – Edinburgh (U.K.), 16.10. – 25.10.2018, Eds.: Jens Karstens, Christoph Böttner, Mike Edwards, Ismael Falcon-Suarez, Anita Flohr, Rachael James, Anna Lichtschlag, Doris Maicher, Iain Pheasant, Ben Roche, Bettina Schramm, Michael Wilson, DOI: 10.3289/GEOMAR_REP_NS_48_2019

For GEOMAR Reports, please visit:
https://oceanrep.geomar.de/view/series/GEOMAR_Report.html

Reports of the former IFM-GEOMAR series can be found under:
https://oceanrep.geomar.de/view/series/IFM-GEOMAR_Report.html

GEOMAR
Helmholtz-Zentrum für Ozeanforschung Kiel

Das GEOMAR Helmholtz-Zentrum für Ozeanforschung Kiel ist Mitglied der Helmholtz-Gemeinschaft Deutscher Forschungszentren e.V.

The GEOMAR Helmholtz Centre for Ocean Research Kiel is a member of the Helmholtz Association of German Research Centres

Helmholtz-Zentrum für Ozeanforschung Kiel / Helmholtz Centre for Ocean Research Kiel
GEOMAR
Dienstgebäude Westufer / West Shore Building
Düsternbrooker Weg 20
D-24105 Kiel
Germany

Helmholtz-Zentrum für Ozeanforschung Kiel / Helmholtz Centre for Ocean Research Kiel
GEOMAR
Dienstgebäude Ostufer / East Shore Building
Wischhofstr. 1-3
D-24148 Kiel
Germany

Tel.: +49 431 600-0
Fax: +49 431 600-2805
www.geomar.de